



Review

Enhancing Disease Diagnosis: Biomedical Applications of Surface-Enhanced Raman Scattering

Malama Chisanga ¹, Howbeer Muhamadali ², David I. Ellis ¹  and Royston Goodacre ^{2,*} 

¹ School of Chemistry, Manchester Institute of Biotechnology, University of Manchester, Manchester M1 7DN, UK; malama.chisanga@manchester.ac.uk (M.C.); D.Ellis@manchester.ac.uk (D.I.E.)

² Department of Biochemistry, Institute of Integrative Biology, University of Liverpool, Liverpool L69 7ZB, UK; Howbeer.Muhamad-Ali@liverpool.ac.uk

* Correspondence: roy.goodacre@liverpool.ac.uk

Received: 15 February 2019; Accepted: 13 March 2019; Published: 19 March 2019



Abstract: Surface-enhanced Raman scattering (SERS) has recently gained increasing attention for the detection of trace quantities of biomolecules due to its excellent molecular specificity, ultrasensitivity, and quantitative multiplex ability. Specific single or multiple biomarkers in complex biological environments generate strong and distinct SERS spectral signals when they are in the vicinity of optically active nanoparticles (NPs). When multivariate chemometrics are applied to decipher underlying biomarker patterns, SERS provides qualitative and quantitative information on the inherent biochemical composition and properties that may be indicative of healthy or diseased states. Moreover, SERS allows for differentiation among many closely-related causative agents of diseases exhibiting similar symptoms to guide early prescription of appropriate, targeted and individualised therapeutics. This review provides an overview of recent progress made by the application of SERS in the diagnosis of cancers, microbial and respiratory infections. It is envisaged that recent technology development will help realise full benefits of SERS to gain deeper insights into the pathological pathways for various diseases at the molecular level.

Keywords: surface-enhanced Raman scattering; biomarkers; multivariate analysis; metabolic fingerprinting; disease diagnosis; cancer; microbes; volatile organic compounds

1. Introduction

In clinical practice disease diagnosis is a critical step towards disease management and acts as an indispensable guide towards appropriate treatment and personalised therapy [1]. The initial stage of disease diagnosis, or differential diagnosis, screens possible disease candidates unambiguously correlated to empirical clinical symptoms. This crucial process involves a systematic and objective analysis and understanding of infection-driven changes in complex metabolic processes highlighted by biological markers (biomarkers) [2]. In addition to stratifying normal biological from pathogenic processes, biomarkers may provide valuable information about severity and stage of disease, drug targets and pharmacological response to therapy [3]. Thus, there is always a growing demand to identify, evaluate and validate disease biomarkers for existing and emerging infections. However, diseases usually have complex pathogenesis and pathophysiology profiles that involve multiple intertwined networks of cellular and molecular changes. To capture this biological and biochemical complexity holistically (e.g., in biofluids, tissues, etc.) indicative of healthy or disease states, intensive high-throughput omics-based analytical procedures are frequently used [4,5]. These aim to identify and characterise multiple biomarkers comprehensively to enhance patient outcomes, disease prevention and drug discovery.

In metabolomics, gas chromatography (GC) screens and separates different metabolites in complex sample mixtures, and mass spectrometry (MS) detects mass-to-charge (m/z) ratios to resolve and identify eluted metabolites [6]. Similarly, genomics, transcriptomics and proteomics techniques, such as antibody-based and liquid chromatography (LC)–MS, are effective modalities for identifying specific patterns in biomarkers and pathophysiological mechanisms within the genome, transcriptome and proteome, respectively [7,8]; we note that LC–MS is also extensively used within metabolomics [9]. Indeed, it is obvious that multiparameter approaches are ideal for biomarker discovery, and have been shown widely to provide systematic and clearer insights to unravel complex metabolic processes and pathways underlying various diseases. Nonetheless, when individual diagnostic and prognostic markers (e.g., metabolites, nucleic acids or proteins) are identified, validated and adopted for routine clinical use, there should be a paradigm shift towards simple, rapid, molecularly specific and sensitive analytics for more efficient detection of biomarkers [10]. Additionally, technically demanding and laborious tools like GC–MS and LC–MS are not cost-effective for diagnosing diseases which lack definitive biomarkers at present, but are frequently detected through disease-specific changes in known biomolecules. Preeclampsia is one example, a pregnancy disorder which is characterised by increased levels of a small subset of molecules, *viz.*, proteins, glucose, uric acid, etc., in human biofluids [11]. Similarly, therapeutic drug monitoring (TDM), which involves routine monitoring and tracking of dose dynamics and bioclearance of prescribed drugs to improve therapeutic efficacy, patient compliance and minimise drug toxicity, requires facile, noninvasive and preferably portable tools with lower running costs per sample analysis [12]. Due to the highlighted need, the 21st century has seen an upsurge in the development of simple and high-throughput laboratory analyses to meet urgent diagnostic requirements in pathology and pharmacology.

Surface-enhanced Raman scattering (SERS) has gained overwhelming attention as a powerful state-of-the-art platform for disease diagnosis at the molecular level due to superior specificity and quantitative sensitivity [13]. SERS is a nanoscale vibrational spectroscopy which combines Raman spectroscopy and plasmonic NPs, to amplify the Raman signals and facilitate trace analysis of clinically useful biomolecules at ambient conditions. Of particular interest now is the emergence of portable handheld Raman systems and reproducible enhancing substrates which are directing SERS for point-of-care (PoC) biosensing. This may overcome biosafety concerns associated with transportation of infectious biological samples to the laboratory especially during an outbreak of highly contagious diseases. Additionally, the inherent selectivity and ultrasensitivity of SERS would enable bespoke clinical diagnostics of subclinical infections like pancreatic adenocarcinoma, which are asymptomatic until the late stage of infection [14].

Since its discovery, SERS has been successfully applied to a wide range of fields including environmental [15,16], antibiotic resistance [17,18], food [19,20] and pharmaceuticals [21,22]. However, it is in the last decade that SERS has become an exciting hypothesis-driven tool for *in vitro* and *in vivo* characterisation of diseases in biofluids, cells or biopsy [23,24]. This is driven by the fact that SERS profiles reveal detailed molecular structure and abundance dynamics which define specific diseases with minimal sample handling. Recently, SERS involving direct mixing of human biofluids and bare NPs yielded promising results for detecting global molecular profiles for diseased and healthy status [25]. Feng et al. segregated blood plasma of patients with nasopharyngeal carcinoma from healthy controls with classification sensitivity and specificity of 90.7% and 100%, respectively [25]. Similarly, Shao et al. applied a noninvasive Raman system equipped with a 785 nm laser, and, based on SERS fingerprints measured from direct mixtures of Ag colloid and serum, cohorts of liver disease and normal subjects were discriminated with the aid of multivariate analysis [26].

Whilst these studies demonstrate the sensitivity of SERS, it should be acknowledged that untargeted analysis of biomarkers in chemically diverse samples is very challenging; given that SERS registers signals of all biomolecules such as proteins, carbohydrates and lipids, present in a clinical specimen [27]. Thus, SERS spectral bands are composites of complex convoluted vibrational modes which are extremely difficult to interpret and employ for targeted therapeutics. Needless to

say, untargeted SERS phenotypic signals do not reveal the structural identity of the actual diagnostic markers in complex backgrounds. We reiterate here that the major analytical strength of SERS in clinical diagnostics typically lies in chemical/molecular specificity in combination with the ultrasensitivity of this technique. On this premise, to realise the maximum benefits of SERS, there is a need to target known biomarkers identified *a priori* by other techniques, such as LC-MS or GC-MS, polymerase chain reaction (PCR), etc. As a case in point, Subaihi and coworkers used reversed-phase LC to separate therapeutic drugs in human urine followed by quantitative detection by SERS [28]. Furthermore, specific disease markers can be detected by SERS method, which has been extensively reported by Graham and Faulds and coworkers [23,29]. Here, SERS signals of target analytes are measured indirectly through SERS-active reporter molecules and recognition elements adsorbed onto NP surface. Notably, Gracie et al. employed AgNPs labelled with a fluorescent reporter and biotin modification probes to detect multiple DNA sequences extracted from etiological agents of meningitis in clinical samples [30], extending on the picomolar quantitative detection of actual meningitis pathogens reported previously [31]. When utilised in this manner, SERS produces unique, sharp and well resolved analyte-specific signature peaks of exceptionally narrow bandwidth and fluorescence-free background. In this context, SERS can provide answers to the 'yes' or 'no' diagnostic questions pertaining to the presence or absence of disease, and importantly, quantitative information based on specific single or multiple biomarkers. Clearly, when used to its fundamental strength, SERS is a very strong candidate for quick and reliable qualitative and quantitative diagnostics and interpretation of novel clinical biomarkers to reveal varying degrees and severity of infections.

The main objective of this focus review is to provide an overview of the current and future utility of SERS as an information-rich and sensitive bioanalytical platform for rapid disease diagnosis based on specific biomarkers. A brief SERS tutorial is given, followed by the description of multivariate chemometrics. Lastly, exciting applications focusing on cancers, microbial and respiratory infections and an outlook on future work focused on clinical translation of SERS is discussed.

2. Surface Enhanced Raman Scattering: A Brief Tutorial

Previously theorised by Smekal in 1923 [32], the Raman effect was discovered and experimentally demonstrated by Sir C. V. Raman in 1928 using simple optical materials and instrumental setup [33]. Raman spectroscopy is a specific optical readout platform which involves scattering of irradiated light following interaction with polarisable molecules under interrogation with a monochromatic laser source. By far the largest proportion of scattered photons has the same energy as incident light (known as Rayleigh scattering), and so does not carry significant chemical information [34]. However, a very small fraction of emergent radiation is inelastically scattered (Raman scattering), with photons of lower frequency than incident radiation (Stokes scattering) being measured in conventional Raman spectroscopy. Raman spectroscopy instrumentation has greatly evolved mechanically and technically over time. Nowadays, powerful and stable lasers, sensitive detectors, optical fibres and software have accelerated the application of Raman spectroscopy in bioanalytical chemistry. Despite this, the scattering cross-section of the Raman Effect is still extremely inefficient with a photon conversion rate of less than 1 per 10^6 – 10^8 incident photons. So to obtain Raman spectra of good signal-to-noise ratio, high power density, long collection time and clinically unrealistic concentrations are usually required. Such measurement parameters often initiate fluorescence and photodegradation which frequently mask Raman spectral lines. This limits the utility of Raman spectroscopy for diagnosis of diseases in biofluids or cells, where biomarkers may be in trace quantities and preserving sample integrity is desirable [29]. It is indeed exciting that significant attention has now shifted to SERS to overcome the quantum inefficiency of conventional Raman spectroscopy.

The SERS effect was discovered accidentally by Fleischmann and coworkers in 1974 at the University of Southampton (UK), when they observed a dramatic increase in Raman signals of a monolayer of pyridine adsorbed onto electrochemically roughened Ag electrodes [35]. At that time, the anomalous observation was thought to be a combined effect of the large surface area of roughened Ag

electrodes and increased local concentration of adsorbed pyridine molecules. This discovery marked the beginning of an excitingly new era of physical and surface chemistry, attracting much attention from analytical scientists and engineers. In 1977, Van Duyne and colleagues [36] and Creighton and coworkers [37] independently concluded that the observed anomaly in Raman signals of pyridine was rather due to increased cross-section as a result of enhanced electric fields induced by roughened Ag electrodes. It was at this time when Van Duyne enlightened the scientific community and coined the term 'surface-enhanced Raman scattering (SERS)' as we know it today.

In principle, SERS involves interactions between electromagnetic radiation and molecules adsorbed onto, or in close proximity to, nanoscale rough metallic particles of smaller diameter than the wavelength of excitation radiation [38]. Although there is no comprehensive explanation for the SERS phenomenon to date, and the topic is under active debate [39], the independent research by Van Duyne and Creighton, combined with selection rules of molecules adsorbed on metal surfaces [40], proposed two simultaneously operative theories. The electromagnetic (EM) theory, thought to be the dominant mechanism, is a physical effect which involves optical excitation of electric fields and charge motions created by collective oscillations of electrons in the conduction band (surface plasmon) of NPs. This interaction creates localised surface plasmon resonance (LSPR), the so-called 'hotspots' around NP surfaces [41]. Therefore, analyte molecules that interact with LSPR and produce intensified spectral signals with enhancement factor (EF) of 10^6 – 10^8 compared to conventional Raman lines. According to the EM theory [42], the SERS intensity (I) is directly proportional to the fourth power of the local electromagnetic field strength (E^4). By contrast, E varies inversely to the distance (d) between analyte and NP surface, that is, $E \propto (1/d)^{1/2}$. Based on these mathematical expressions, EM is distance-dependent, and small modification in d and E results in exponential changes in I . Ideally, the optimum SERS is achieved when an optimal number of analytes are within regions of strong LSPR, within the interstices of aggregated NPs [43].

The second, chemical enhancement (CM) or charge-transfer mechanism relies on resonance Raman scattering-like effect. It is thought to involve electronic excitation of covalently bound coupled electron clouds within chemical bonds formed between analytes and the NP surface. CM increases polarisability of adsorbed molecules and contributes up to 10^3 orders of magnitude to the overall SERS EF [43]. Unlike EM, CM is only significant when molecules are chemically bonded to NPs typically at monolayer coverage. It is also noteworthy that the Raman effect can be tuned further to 10^{14} orders of magnitude to reach fluorescence-like cross-section [44]. This is achieved when incident frequency excites electronic energy states of specific chromophores near or bonded to the NP surface, giving rise to surface-enhanced resonance Raman scattering (SERRS). With this large EF, ultralow limit of detection (LOD) to the extent of single molecule detection were reported by Kneipp and coworkers [45]. Overall, to achieve this optimally huge SERS amplification, several experimental parameters need to be manipulated including laser wavelength, morphology of NPs and dispersion medium. For more detailed information on experimental considerations for optimal SERS, readers are directed to excellent reviews by Stiles et al. and Fisk et al. [42,46]. Quite importantly, optimally aggregated NPs, excitation frequency overlapped with plasmonic band of NPs and enhancing media with small refractive index collectively yield large and reproducible EFs [47]. In terms of technical aspect, flow injection and microfluidics technologies combined with SERS show good SERS reproducibility and reliability [48]. Microfluidics devices consist of microchannels where a minute volume of a sample is mixed uniformly with NPs at constant and automated flow velocity. Tandem microfluidics-SERS overcomes effects of localised heating, photodissociation and variations in scattering geometry of NPs. A considerable focus of recent research has been on developing microfluidic SERS to improve in situ bioanalysis, which will play a decisive role for clinical utility of SERS in healthcare systems [49].

3. The Affinity of SERS-Active Substrates for Biochemical Molecules

Currently, there is a wide range of solid and dispersed substrates used as SERS enhancement media ranging from roughened metals to thin metal films to colloidal NPs. Colloids based on coinage

metals—Ag and Au—are predominantly used in bioanalytical science partly due to ease of preparation and modification, low-cost, high stability and large EF [50]. Also, Ag and Au nanomaterials exhibit naturally high affinity for molecules that possess highly electronegative or charged atoms (e.g., oxygen, nitrogen, sulfur, etc.). Interestingly, numerous biomarkers such as metabolites, nucleic acids and proteins (the reactants, intermediates and end products of genetically encoded processes), contain one or more electronegative atoms and polarisable delocalised π -conjugated system and so they have strong SERS activity [51,52]. Moreover, since molecular symmetry properties change when molecules are bonded to the NP surface, centrosymmetric biomolecules are detectable by SERS. Thus, SERS has unlocked new prospects to apply unique diagnostic information obtained from symmetrical biomarkers, which would otherwise not be amenable by Raman or Fourier-transform infrared (FT-IR) spectroscopies, according to the mutual exclusion principle [52].

In general, there are two approaches to accomplish SERS measurements namely, label-free and label-based techniques as shown in Figure 1. Label-free or intrinsic SERS measures direct interactions between analytes and NPs [53]. The resultant spectral bands provide detailed intrinsic structural information and dynamics in biomolecules directly attached to NPs. By contrast, label-based or extrinsic SERS combines optical activity of plasmonic materials (Ag, Au, Cu, etc.) functionalised with SERS-active messenger molecules (so-called Raman ‘reporters’), which are resonant with a wide range of available excitation lasers [30]. The recognition element, e.g., antibody, enzyme, aptamer, etc., attached to NP surface binds to epitope(s) of specific target analytes (e.g., a metabolite, nucleic acid or bacterium) and its plasmonically enhanced characteristic SERS signal is measured indirectly through the Raman reporter. When several biocompatible recognition elements are employed, extrinsic SERS offers quantitative multiplexed analysis of biomarkers in complex fluid matrices.

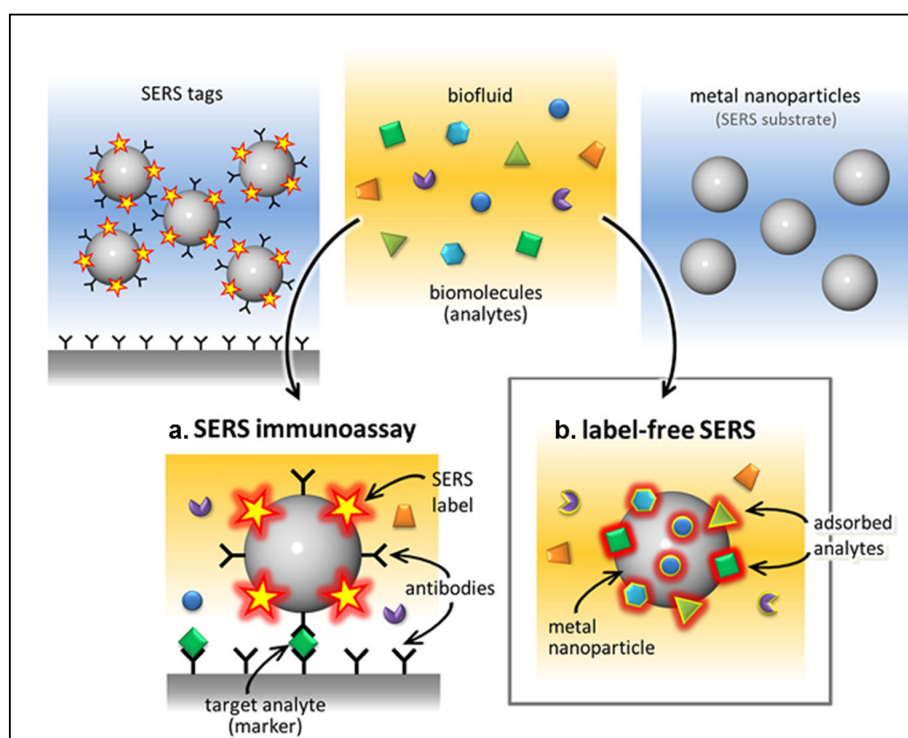


Figure 1. Surface-enhanced Raman scattering (SERS) approaches: a. label-based (extrinsic) and b. label-free (intrinsic) SERS. Reproduced with permission from Bonifacio et al. [54]. Copyright © 2015, Springer Nature.

4. Multivariate Chemometrics

The SERS spectra obtained from biological samples are multivariate in nature. That is to say, they consist of thousands of complex and combination vibrational modes which are difficult to interpret

by simple stare & compare. The fundamental tenet of multivariate analysis (MVA) is to simplify multivariate data systematically to a small number of variables whilst preserving maximum variance within a data matrix to guide scientific reasoning. This is accomplished through unsupervised and/or supervised MVA (machine learning) modelling.

Unsupervised MVA explore natural variance within a data matrix using spectral variables in vertical columns (the X -data) as the only input data measured from objects in horizontal rows (the Y -data) of a data matrix. Principal components analysis (PCA) is a widely used traditional, unsupervised approach to reduce data dimensionality, classify spectra into specific groups and to identify outliers [55]. In principle, PCA decomposes multivariate data into scores (clusters) and associated spectral loadings. The scores plots consist of uncorrelated orthogonal hyperplanes called principal components (PCs), which display the differences, similarities and the total explained variance in the dataset; e.g., cancerous *vs.* noncancerous conditions. PC1 is extracted from the input X -data to account for the largest variance, whilst PC2, PC3, . . . PC n (where n is an integer), explain the remaining natural variance in decreasing order. The PC loadings spectra are plotted to highlight the most important input spectral variables responsible for the clustering pattern observed on a PCA scores plot. In the case of disease diagnosis, the variables on a loadings plot often denote intensity ratio differences and/or spectral band shifts between diseased and healthy groups. Since PCA does not rely on prior knowledge of investigated samples, it is *exploratory* by nature which implies that the algorithm can discover novel hidden biological patterns within samples under review, and is very useful for outlier detection [56]. Other unsupervised models are dendrograms, self-organising maps, autoassociative neural network, etc. By contrast, supervised models are calibrated with a known response variable(s) (the Y -data) to act as building blocks for supervised algorithms.

Discriminant analysis and partial least-squares regression (PLSR) are commonly used supervised models for classification and quantitative predictions of SERS spectral data [57]. Discriminant function analysis (DFA) combines PCs extracted from the X -data and *a priori* knowledge: e.g., sample objects (classes) in the Y -data to minimise within-class and maximise between-class variance for classification purposes. On the other hand, PLSR has proved to be powerful and useful in *quantitative* analysis of biomarkers by SERS, which employs correlated variables in both X - and Y -data to build a linear relationship. For PLSR modelling, the sample spectral dataset is first divided into two parts: the training and test sets. The first subset of sample spectra are used to calibrate or train a PLSR model followed by quantitative prediction of the remaining unseen samples in the test set [58]. A PLSR model of good quality or performance will aim to generate a correlation coefficient (R^2 or Q^2 for trained and tested sets, respectively), which is close to one and low root mean squared error (RMSE). Partial least-squares-discriminant analysis (PLS-DA), a variant of PLSR, is also a very powerful multivariate model particularly applied when the Y -data are categorical by nature [59].

In addition to these linear discriminant analysis methods there are several nonlinear equivalents that effect nonlinear mapping from input X -data (spectra) to output Y -data (the classes or sample objects). These are often referred to as machine learning techniques and perhaps the most popular are support vector machines (SVMs), random forests (RFs) and kernel PLS (kPLS): these are reviewed in Gromski et al., Mazivila et al., Shinzawa et al., and Ellis et al. [59–62]. The recent resurgence of interest in artificial intelligence and artificial neural networks (ANNs) has given rise to deep learning. In these convolution neural networks many different layers are used [63], which are fundamentally different to the single layer neural networks developed by Rumelhart and colleagues [64]. These have predominantly been used for image analysis and speech recognition and they are very data hungry (that is to say require lots of input data) and may have a role in the analysis of chemical images generated from SERS and Raman microspectroscopy as illustrated by Shi et al. and Krauss et al. [65,66].

As the old saying reveals—“you will reap what you sow”—if a supervised model is incorrectly calibrated, there is a possibility of overfitting and subsequently false classification or regression. For accurate prediction, quality control and assurance in disease diagnostics, it is always important that the number of latent variables is selected carefully and supervised models are validated through bootstrapping or n -fold cross-validation, etc. [67].

Examples of where chemometrics has been applied to SERS and related techniques include detection of cancers using PC-LDA and SVM [68–71], microbial pathogens by various discriminant and cluster analysis [72–74] and drug and their metabolites by PLS and ANNs [75–77].

5. Applications of SERS in Disease Diagnostics

5.1. Cancer

Cancer is a major public health concern and an economic burden globally. Recent research indicates that 17.5 million cancer cases were recorded worldwide in 2015, culminating in 8.7 million deaths [78]. Unfortunately the number of cancer cases increased sharply after two years in 2018 making cancer the second most common cause of death worldwide [79]. Cancer is a collective term used to describe malignancies characterised by rapid abnormal growth of cells which invade other parts of the body. At the onset of cancer, specific biochemical molecules (e.g., proteins) are elevated or decreased in cancer patients and such dynamics serve as biomarkers for various types of cancers [80]. The early diagnosis of cancer, especially before metastasis, correlates well with the effectiveness of therapy, improved patient survival rates and prognosis. To this end, significant effort has been devoted towards the development of molecular biosensing platforms in recent years to meet the ever-demanding diagnostics of cancers in human cells, tissues and biofluids. Among these, immunoassays exhibit considerably high sensitivity and so they are commonly used as noninvasive strategies to measure biomarkers based on antibody–antigen interactions at different stages of cancer development [81].

The early work to highlight the diagnostic potential of immunoassays used radioisotopes to label antigens and antibodies to trace dynamics in target markers and metabolism indicative of cancers [82]. Unsurprisingly, the use of radioisotope immunoassay (RIA) in clinics declined due to environmental health and safety hazards, in addition to costly specialised laboratory facilities and waste disposal routes for radioactive materials. Enzymes are now commonly used as reporters in the enzyme-linked immunosorbent assay (ELISA). ELISA is safer, simpler, rapid and the gold standard assay used for routine analysis of protein cancer biomarkers. Several authors have documented the utility of ELISA in cancer studies [83,84]. For instance, Ambrosi et al. detected low levels of CA15-3 glycoprotein antigen mainly observed in patients with breast cancer using anti-CA15-3–horseradish peroxidase conjugate chemically bonded to an Au solid substrate [85]; whereas Fitzgerald et al. investigated colorectal cancer by accurately measuring autoimmune responses of IgM and IgG antibodies in human serum [86]. Nonetheless, long analysis times and high cost of commercial ELISA test kit limit the application of ELISA. Alternatively, fluorescence-based portable biosensors are well developed and extensively applied as readout assays. In terms of quantum yield, fluorescence has a large absorption cross-section, thus fluorescent immunoassay (FIA) has excellent sensitivity which enables detection of cancer biomarkers at clinically desirable LODs [87,88]. However, FIA has several drawbacks: difficulty with labelling recognition or target species, limited multiplexing due to frequent spectral overlap caused by broad emission bands, as well as photobleaching and nonspecific binding, especially at low analyte levels.

SERS has vital advantages over traditional immunoassays used in clinical biochemistry: it exhibits multiplexing ability with a single excitation laser and ultrasensitivity leading to absolute quantitative detection [10] and, if optimized, correctly rivals gold standard assays. Recently, reproducible substrates based on antibody-conjugated hollow Au nanospheres and magnetic beads were applied for rapid sensing of carcinoembryonic antigen (CEA)—a biomarker of lung cancer [89]. In this study, the SERS assay detected low amount (1 pg/mL) of CEA accurately, which was 1000-fold more sensitive than ELISA. Since the amount of CEA is clinically determined to be about 10 ng/mL in malignant cases [80], SERS detected subinfectious regime suitable for monitoring and predicting inception of lung cancer to avoid increased risk of severe metastasis. In subsequent studies, attention shifted towards *ex vivo* analysis of human biofluids to test novel biosensors in real biological environments. Within this framework, Wang et al. analysed diagnostic and prognostic markers of pancreatic cancer, mucin

(MUC4) protein and serum carbohydrate (CA-19-9) antigen, and compared SERS results to ELISA and RIA [90]. In addition to quick readout time, SERS demonstrated much better sensitivity (LOD 33 ng/mL) than ELISA (LOD 30 $\mu\text{g/mL}$) for MUC4, and an LOD of 0.8 U/mL compared to RIA's 1.0 U/mL for CA-19-9. Interestingly, SERS quantified trace levels of MUC4 in human serum for pancreatic cancer patients whereas ELISA and RIA failed to register signals under same conditions. Many other articles have appeared showing that SERS is also versatile as it can detect various cancers both in vitro and in vivo [91–94].

The last decade has seen substantial progress directed towards the application of SERS for detecting multiple disease markers simultaneously aimed to reduce risks of false positives associated with singular biomarker detection and to strengthen differential diagnostics. One of the earliest multiplexed assays was reported by Faulds, who identified five DNA sequences (5-plex) quantitatively at 1 pM detection limit within a single assay [95]. Quite recently, a similar sensitivity regime was reported for prostate-free prostate specific antigens (f-PSA) and complexed prostate specific antigens (c-PSA) [96] and pancreatic CA19-9, matrix metalloproteinase-7 (MMP7) and MUC4 [97], cancers in 2-plex and 3-plex in human serum, respectively. The multiplex SERS method shown in Figure 2 of the former study, proposed a very sensitive and selective sandwich immunocomplex (SIC) nanotags, similar to those reported in recent years [98,99]. The robust and specific SIC assay showed negligible nonspecific binding and cross reactivity between f-PSA and c-PSA [96]. This represents a remarkable leap toward reduction of false positives and assay non-reactivity driven by random binding to interferents which hamper the vast majority of diagnostic immunoassays. More important, the computed values of free to total PSA ratio for clinical samples clearly indicated that optimal dual-binding SERS assay can match the sensitivity of chemiluminescence standard used in clinics.

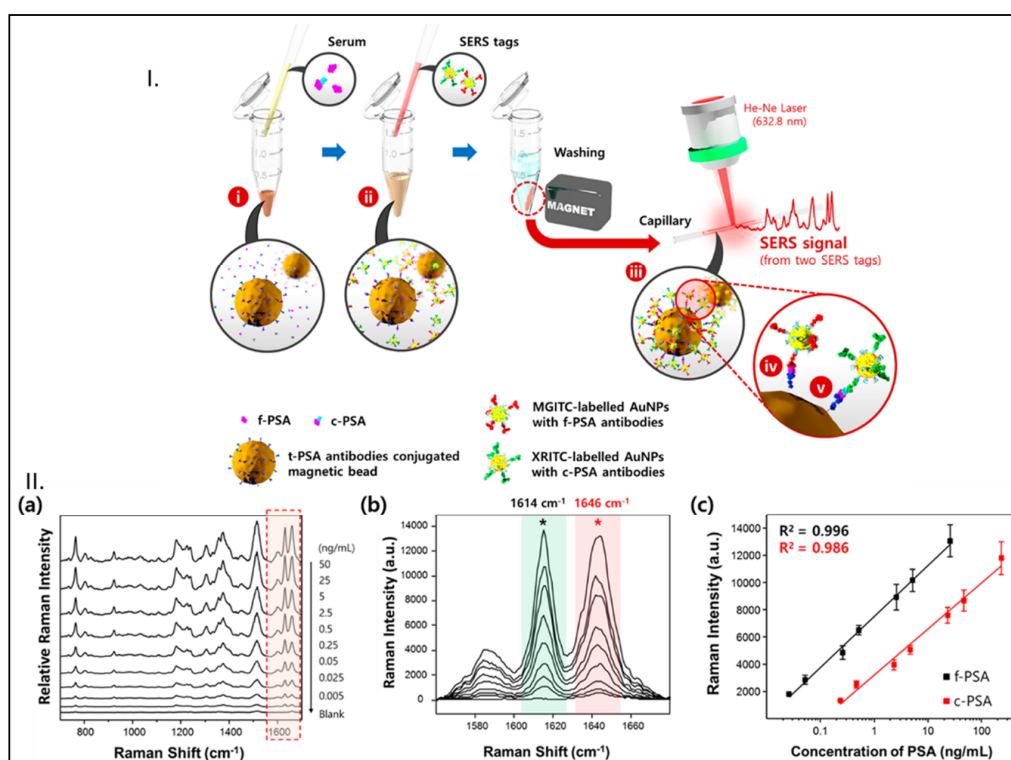


Figure 2. (I) Schematic illustration of SERS immunoassay approach for multiplex detection. i. analytical mixture of free-prostate specific antigens (f-PSA) and complexed prostate specific antigens (c-PSA) with antibody-conjugated magnetic beads, ii. formation of sandwich immunocomplex (SIC) upon addition of SERS nanotags, iii. magnetic separation of immunocomplexes and iv. and v. simultaneous detection of f-PSA and c-PSA in serum, respectively. (II) Quantitative analysis (a) and (b). Characteristics SERS spectra at different concentrations for f-PSA and c-PSA. (c) Corresponding calibration curves. Reprinted with permission from Cheng et al. [96]. Copyright © 2017, American Chemical Society.

Huge efforts have also been made to deploy automated digital microfluidics-SERS for on-site biosensing of multiple cancer protein markers in minute sample volumes. Recently, a simple prototype microfluidics-SERS, with minimal sample processing, detected subinfective dose of prostate cancer [100]. Nguyen et al. and Perozziello et al. quantified breast cancer biomarkers at 6.5 fM in serum [92] and 0.1 ppm in plasma [101], respectively. The latter study demonstrated a novel sensor for rapid sorting and quantitative detection of peptides which may play a vital role where multiplexed analysis tends to be complicated by intermolecular interactions between analyte biomarkers. Other researchers have gone so far as to suggest multiplex PCR-SERS to study melanoma DNA mutations associated with various cancers [102]. By combining the biochemical superiority of PCR, and the sensitivity and specificity of SERS, mutant alleles as low as 0.1% could be identified in serum. This illustrates the potential of PCR-SERS to guide important clinical decisions regarding tumour biology with respect to heredity, diagnostics and treatment.

5.2. Microbial Infections–Pathogen Detection

Microbes are found everywhere in large quantities and complex consortia where they perform specialised functions that play a vital role in ecosystems on which humans depend—quite often within the superorganism host [103]. However, it is well known that a small proportion of microbes such as bacteria, fungi and protozoa are responsible for foodborne, waterborne and tuberculosis which contribute to high mortality and morbidity rates globally [104]. Although local and international guidelines for combatting diseases are available, microbial infections are still unacceptably high worldwide with a significant burden borne by the developing world. Just recently perhaps the largest outbreak of listeriosis, a foodborne infection contracted through consumption of food contaminated with *Listeria monocytogenes* bacterium, which occurred in South Africa [105]. The number of affected confirmed laboratory cases was estimated at 674 with 183 deaths recorded. On the other hand, waterborne infections are reported to be associated with gastroenteritis cases that claim 2 million deaths per year globally, and the number of deaths is likely to increase every hour that therapeutic treatment is delayed [106]. At the time of writing this review, it was reported that at least 54% of chicken meat sold in Germany supermarkets and 79% of those in slaughter houses were contaminated with *Campylobacter* spp. pathogens [107]. Due to the dramatic increase in incidence rates driven by quick transmission, spread and antimicrobial resistance (AMR) of acute infections, there is an urgent demand for rapid and ultrasensitive tools to characterise pathogens to protect public health and to prevent potential bioterrorism. Furthermore, unequivocal identification and differentiation of pathogens, especially at the PoC, will certainly offer an opportunity to trace the origin of fatal sporadic infections in order to design effective immediate and long-term corrective action.

Until very recently, routine microbial diagnostics were dominated by traditional platforms based on culturing, biochemical tests and colony counting [108]. However, these methods are inherently time-consuming, laborious and centralised (i.e., tests are done in dedicated laboratories rather than on site), as well as sometimes being inapplicable depending on pathogenic species under investigation. For example, bacteria such as *Mycobacterium tuberculosis* may take several days to weeks to form visible colonies, while selective *Campylobacter* spp. are biochemically unreactive [109,110]. Alternatively, immunoassays and molecular tools based on ELISA and PCR have shown much improved rapidity and applicability [111,112]. These techniques have better detection limits, offer accurate phylogenetic identity and classification and allow for simultaneous detection of multiple pathogens provided several antibodies or primers are employed. Although ELISA and PCR have found extensive use in clinical diagnostics they are costly, labour-intensive, require trained personnel and have long turnaround times necessitated by pretreatment and enrichment steps. PCR in particular is prone false positive tests due to cross contamination from the environment and during sample collection, omits phenotypic characteristics of pathogens and fails to differentiate viable from nonviable infectious pathogens since the genetic material is always present in live or dead microbial cells. Moreover, the analytical merit of PCR based on exponential amplification of genetic materials can be a devastating disadvantage in case of sample contamination [108].

To bridge the gap, intrinsically robust SERS protocols with little or no sample preparation could be applied widely for reliable and noninvasive biosensing of microbial infections. The objective of using SERS is to obtain unique “whole-organism” metabolic fingerprints to discern intrinsic biochemical content and dynamics of microbial cells. The differential characteristic SERS frequencies of chemical bonds are used to identify, discriminate and define phenotypes of infectious microbes at species and strain levels in just a few minutes, as demonstrated previously [18,113]. Of the successful applications of SERS for microbial diagnostics, the report by Jarvis and Goodacre was the first to study urinary tract infection (UTI) [72]. In this study, 21 clinical isolates responsible for UTI, including *Escherichia coli*, *Enterococcus* spp., *Klebsiella pneumoniae* and *Proteus mirabilis*, were identified and classified accurately at species and strain level without recourse to DNA methods. To solve reproducibility problems linked to the simple mixing method applied by Jarvis and other authors [72,114,115], Shanmukh et al. developed robust clinical grade fabricated solid Ag nanorods to classify molecular signatures of respiratory syncytial virus (RSV) associated with bronchiolitis [116], whilst Chen et al. proposed aggregated Au/AgNP covered SiO₂ solid substrates to detect phenotypes of resistant etiological agents of sexually transmitted infections (STIs) in just 10 s [117]. In a further analysis, SERS was extended to diagnosis of aggressive fungal diseases, in order to discriminate among dermatophyte fungi strains responsible for mycotic infections using reproducible commercial Ag-coated NPs [118].

Recently, novel SERS employing in situ synthesis of NPs, wherein microbial cells act as templates for nucleation of NP, has shown much improved reproducibility of the detected microbial SERS signal. In this method when active microbial cells are soaked in an oxidant (e.g., AgNO₃), metal cations are attracted to anions within cellular biomolecules to act as coordination centres. A reductant solution (e.g., NaBH₄) is then introduced to reduce coordinated metal cations to form cell wall-bound monodispersed NPs [119,120]. Intracellular deposition of NPs can also be achieved when oxidants and reductants are added in a reverse order [120]. This approach enhances clinical applicability of SERS as demonstrated for accurate identification and classification of clinical isolates of *E. coli*, *Bacillus* spp. [120,121], opportunistic *Staphylococcus epidermidis* [17], *Aspergillus fumigatus* and *Rhizomucor pusillus* [122], and to probe microbial cell functionality [119]. Intriguingly, an in situ SERS method proved to be very sensitive and effective for susceptibility assessment of clinical pathogens against common first line antibiotics treatment [17], to complement previous efforts [18,123]. AMR is considered as one of the biggest public health threats where microbes elude antibiotics designed to kill them. AMR makes it difficult or impossible to treat some invasive microbial infections. To improve the management of endemic AMR, Zhou et al. developed a sensitive SERS biosensor to detect biochemical signatures and status of bacterial infections and AMR rapidly [17]. This SERS biosensor not only enumerated cells to assess infection severity but also distinguished live (resistant) from dead (sensitive) *E. coli* cells challenged with antibiotics based on differential spectral signatures as illustrated in Figure 3; a result which is practically impossible to achieve by DNA tools like PCR [108]. Whilst lengthy conventional culturing methods can also differentiate live and dead cells for cultivable organisms, it gives false negative results for viable but non-culturable pathogens.

The practical advantage with SERS here is that unlike in dead cells, metabolically active microbes can incorporate NPs to their biomolecules in the cell envelope or cytoplasm more effectively that provide larger and distinctive EF shown in Figure 3. This provides access to vital information about microbial viability state which is invaluable for tracking the response of causative microbes to prescribed antimicrobial therapy. Apparently the short time at which AMR was detected in this study [17] may help to prevent or cure opportunistic infections during surgeries and organ transplants, and to avoid the use of broad spectrum antibiotics which contribute to increase in AMR. In the coming years, in situ SERS needs validation through multicentral tests for AMR in a large cohort of clinical isolates and antibiotics using standardised protocols. Also, the Raman vibrational modes for heavy water (D₂O) are well established [124], and several authors have probed the general metabolic activity of microbial community members capable of degrading environmental contaminants [124,125]. Similarly, D₂O can be incorporated to AMR studies to probe the metabolic activity of sensitive and

resistant microbes for in-depth assessment and elucidation of bactericidal and bacteriostatic effects of common and novel antibiotics. Since SERS spectral data provides information on the structural properties of biomolecules, probing cells with D₂O in a time course fashion may identify novel (multi)-resistant prokaryotes, offer kinetics and mechanistic insights into AMR and treatment prognosis. In addition, it may reveal valuable biochemical changes in pathogens due to the regulation of drug metabolism to guide the next generation therapeutics.

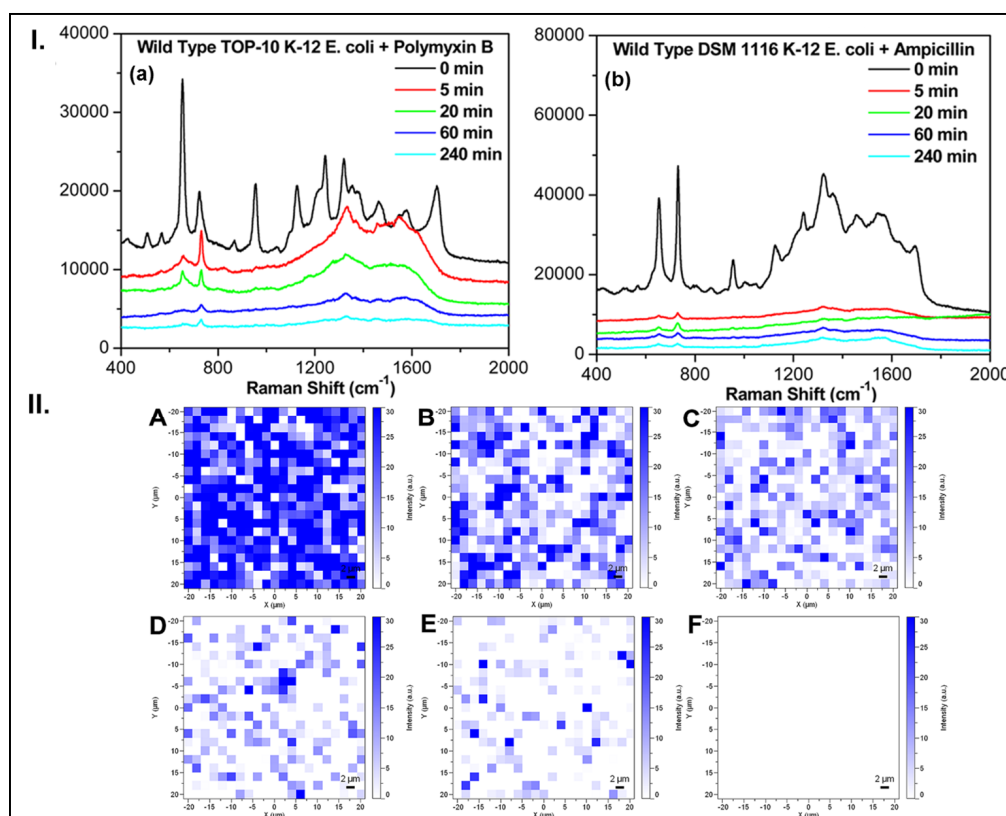


Figure 3. (I) In situ SERS spectral profiles of sensitive wild type *E. coli* K-12 TOP-10 and K-12 DSM. Strains ($n = 116$) treated with (a) Polymyxin B and (b) Ampicillin, harvested at different time points. By visual inspection, the intensity of SERS bands decreased while new bands appeared with increasing time in both cases. (II) SERS images showing increasing concentrations of dead *E. coli* cells, A. 0%, B. 5%, C. 25%, D. 50%, E. 75% and F. 100%, quantified by 735 cm^{-1} band, clearly indicating that no SERS signals were detected on dead cells. Colour code: Blue = live cell and white = dead cell. Reprinted with permission from Zhou et al. [17]. Copyright © 2017, American Chemical Society.

The label-free SERS approach can also be complemented by label-based SERS to allow high-level multiplexed analysis of pathogens in patient samples. Renishaw Diagnostics recently developed a cutting edge robust SERS-based multiplex tool called Fungiplex assay [126]. This is perhaps the greatest milestone in recent years which has pushed SERS toward routine clinical use. In its trial phase, a Fungiplex assay reproducibly detected and identified blood-derived DNA for 12 *Candida* and *Aspergillus* pathogens ex vivo in a single run. Following this, several researchers have launched ultrasensitive assays of clinical quality for the isolation and quantitative detection of antibiotic resistant bacteria at 10 cfu/mL [73], DNA of meningitis-associated pathogens at $\sim 21\text{ pM}$ [31], viruses at 10 pg/mL in serum [127] and deadly Ebola virus in blood [128], in 3-plexed analysis, to confirm the potential of SERS to meet workflow demands for real-time PoC diagnostics. When coupled to rapidly emerging novel devices—lab-on-a-chip [129,130], microbial- and nano-barcoding [131,132]—SERS has better stability, ruggedness and analytical performance. This makes SERS undoubtedly exploitable for

in-field investigations of multiple conflicting coinfections in vivo, especially in remote areas which are highly susceptible to outbreaks of communicable diseases [128].

5.3. SERS in Breath Analysis

Breathomics is defined as the metabolomics of exhaled air. Human exhaled breath predominantly consists of water, oxygen, nitrogen, nitric oxide and carbon dioxide. In addition, it contains thousands of small gaseous volatile organic compounds (VOCs) which are produced by numerous and highly regulated metabolic reactions in various metabolic pathways [133]. Since the structural identity and abundance of endogenous VOCs vary depending on the health status of an individual, the field of breathomics has much potential as a powerful noninvasive platform for biomarker discovery. Moreover, since each patient produces unique characteristic VOC signatures for specific illnesses, breathomics will potentially play a crucial role in personalised medicine [134]. Despite attracting increasing attention, the progress of breathomics research for clinical diagnostics is relatively slow partly due to limitations associated with capture of breath, and selective and sensitive detection of trace quantities of VOCs [135].

Electronic nose (eNose) technology is an emerging portable tool for pattern recognition in composite responses of mixed VOCs (breathprint). Although eNose provides breathprints that can be used to detect asthma and chronic obstructive pulmonary disease (COPD) [136], it does not identify individual VOC markers within a complex mixture. Ion mobility spectrometry (IMS) is a relatively sensitive method though it is destructive, may not be ideal for complex VOC mixtures and its long term reproducibility is yet to be demonstrated [137]. Currently, GC-MS is the gold standard for global profiling of exhaled VOCs related to abnormal metabolism and extrapolated to cancers, diabetes etc. However, if the goal is to develop a rapid analytical tool for online diagnostics and/or offline use in real-time at the PoC especially in low income countries, then GC-MS is perhaps not convenient. In addition as partly stated earlier, GC-MS requires professional operators, lengthy procedures, and high instrument maintenance and consumables costs. This is where SERS prevails in clinical practice to offer low-cost but quicker detection of disease-specific singular or multiplex VOC targets directly in exhaled breath at a point of need. The fact that both exogenous and endogenous VOCs are present at trace concentrations in exhaled breath; SERS is an exciting prospect as it may allow for the detection of any VOCs adsorbed onto nanomaterials, down to single-molecule level [138].

Although SERS as a clinical diagnostic tool for breath analysis is currently at the budding stage, the results obtained so far shows unprecedented potential. Initial proof-of-concept work aimed to detect low amounts of pure acetone and ethanol vapour at LODs of 3.7 pg and 1.7 pg, respectively, as singular or duplex markers of glucose level in plasma [139,140]. Nevertheless, due to complex pathogenesis associated with breath-related infections, where multiple biochemical and cellular processes are linked to innate and adaptive mechanisms, human exhaled breath is chemically complex. Hence, VOC components should be 'sorted out' to improve pathophysiological assessment of various diseases. An interesting study by Chen et al. was initially applied a high-throughput GC-MS, to capture this biological complexity, and SERS in parallel, to discriminate between early and advanced gastric cancer (EGC and AGC respectively) from healthy controls [141]. Using GC-MS and solid phase microextraction, 14 characteristic volatile metabolites were screened and identified in human exhaled breath. SERS based on in situ synthesised AuNPs coated on graphene oxide then detected individual profiles for all 14 VOCs rapidly and accurately in both simulated and real exhaled breath sampled from patients of gastric cancer. PCA scores plot of SERS successfully discriminated healthy, EGC and AGC in 200 breath samples at diagnostic sensitivity of >92% and specificity of >83%, very comparable to that of GC-MS, though quantitative characterisation was not demonstrated [141]. It is worth noting that SERS profiles were unaffected by age and gender of patients, illustrating the ability of SERS to overcome effects of between-patient confounding factors in routine clinical tests.

A key prerequisite for successful SERS application in breath analysis is the design of optically sensitive probes that 'arrest' and provide a large surface area for adsorption of volatile metabolites

since VOCs diffuse quickly according to the Graham's law [142]. Several SERS substrates with improved capture properties have been proposed including bimetallic nanogaps [139,143], dendritic nanocrystals [144] and 3D multilayered nanowires [143]. However, a SERS biosensor designed by Qiao et al. (Figure 4), where aggregated spherical Au superparticles (GSP) coated with ZIF-8 (so-called GSP@ZIF-8) formed a 3D core-shell to act as a SERS-active substrate and metal organic framework (MOF) that is quite attractive [145]. The notable merit of the GSP@ZIF-8 3D structure sensor is the ability to slow down the flow rate to promote adsorption, retention and equilibration of VOCs, resulting in increased enrichment and reproducibility. Clearly, GSP@ZIF-8 biosensor is more appealing and feasible for clinical analysis of specific lung cancer VOC biomarkers in real-time at the point of need.

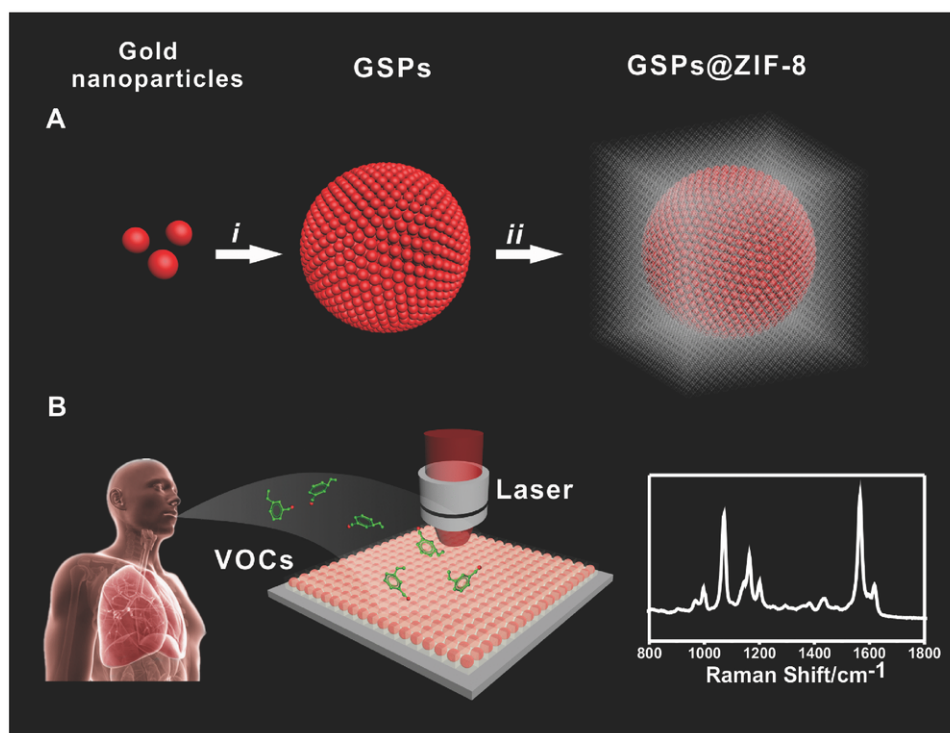


Figure 4. (A) Synthetic route for GSP@ZIF-8 3D core-shell. i. Aggregation of gold nanoparticles (AuNPs) to form spherical GSP. ii. GSP surface-coated with ZIF-8 shell. (B) Exhaled breath capture on GSP@ZIF-8 3D core-shell and detection of VOCs markers by SERS. Reproduced with permission from Qiao et al. [145]. Copyright © 2018, John Wiley and Sons.

Recently, SERS has also become popular for the identification of validated headspace VOCs produced by specific invasive pathogens. Bacterial VOCs within exhaled breath or culture headspace are distinct, and their selective recognition serves as biomarkers for chronic illnesses [146]. The chemical structures and identities of a large number of microbial VOCs (mVOCs) biomarkers produced by human pathogens are available in mVOC database [147]. Hydrogen cyanide emitted by *Pseudomonas aeruginosa* associated with cystic fibrosis [148], isovaleric acid for *Staphylococcus aureus* and ethyl acetate and indole linked to sepsis [149], have all been detected and quantified accurately by SERS [150], to supplement recently published results using MS [151,152]. Finally, SERS has been developed to probe the headspace of bacterial cultures to differentiate accurately viable cells from dead bacteria after treatment with the antibiotic gentamicin [153]. Henceforth, such VOC biomarkers will be identifiable in new patients with the same infections. It is very clear here that SERS offers dual benefits for healthcare: the rapid and sensitive detection of actual microbial pathogens and their phenotypic characteristics down to a single cell and the corresponding VOC molecular signatures as confirmatory results simultaneously.

6. Conclusions and Future Outlook

In this review, we have discussed recent applications of SERS and shown that this method is a versatile physicochemical tool that can be used to extract diagnostic and quantitative information within cancers and microbial infections, as well as in respiratory disease. Both direct and indirect SERS play vital roles in targeted detection of specific biomarker in cells or human biofluids and their use have been extended to several diseases in need of urgent attention. However, to harness full analytical capabilities and to accelerate translation of SERS to the clinic, there are pending technical and methodological issues that need urgent improvements. We know very well that SERS peak intensity or area is linearly proportional to the concentration of sample analytes which facilitates accurate quantitative detection of diseases. However, due to saturation of NP surfaces in label-free SERS, whereby some molecules reside outside the LSPR, or instability of a radiation source and inconsistent cumulative aggregation, reproducibility and linearity are lost. To overcome this problem in quantitative analysis, a suitable internal standard (IS) can be integrated so that characteristic biomarker bands are normalised to distinct IS peak. This reduces spectral signal fluctuations since analyte and internal standard spectral bands are affected in exactly the same way, especially when isotopologues are used as illustrated recently [154,155]. Alternatively the standard addition method can be used as this also accounts for any sample background as shown for the quantification of uric acid in the urine of pregnant individuals [156]. This way quantitative detection and prediction of disease/prognostic markers in a clinical environment would be more accurate and reliable. One other area which perhaps needs more attention to simplify SERS interpretation is the use of functionalised NPs (label-based SERS) for selective detection of specific markers within complex backgrounds. It is worth noting that reporters and capture species prevent undesirable aggregation of NPs and resolve known multiple biomarkers simultaneously without any prior separation or enrichment procedures.

The use of SERS in parallel with multiparameter tools is also showing promising trends; it is clear that SERS has improved time between diagnostics and cure, specificity and quantitative analysis of biomarkers identified by chromatography and spectrometry. Moreover, several problematic issues, due to nonspecific binding or cross-reactivity among untargeted species, NPs and capture elements, especially polyclonal antibodies, which hampered detection of desirable targets, have been addressed in recent years. Generally, a series of washing steps and biocompatible coating materials such as polymers and silica as protective layers or core/encapsulation-shells have been applied successfully. The main objective here is to prevent leaching of Raman reporter and capture probes, enhance specificity and to shield interfering contaminants from accessing NP surfaces and paratopes of capture elements.

Another fundamental area of focus for reliable interpretation of biomedical SERS in future is spectral band assignment. For bacterial SERS, metabolomics and isotopic labelling experiments have played an indispensable role; we now understand significant contributions of purines and pyrimidines to characteristic SERS spectral bands [157,158]. Nonetheless, there is still a pressing need to formulate standard operating protocols and a unified library of reference biomaterials for SERS to allow for repeatability, unambiguous and detailed understanding of molecular dynamics and metabolic pathways. In light of this, it should be emphasised that only when pending problems are effectively overcome will SERS be convincingly relevant and acceptable to clinicians. For now the SERS community should aim to provide experimental details including sample preparation, NP synthesis/properties (e.g., plasmonics and morphology), how NPs and analytes are brought into contact, excitation wavelength used, signal acquisition parameters and data processing employed, as part of the minimum reporting standards.

Lastly, theranostics is an emerging interesting area of clinical diagnostics where SERS will play a crucial role as revealed by recent reports [159]. Theranostics combines diagnosis of disease and therapeutic treatment simultaneously. Ag- and Au-NPs have high optical activity and large surface area for functionalisation, and so they are attractive for diagnosis of specific diseases, photothermal therapy and TDM. This means that NPs can provide large optical enhancement and rapid quantitative assessment of disease at trace amounts whilst delivering therapeutic drugs to intended targets. Due to

good biocompatibility, AuNPs can migrate across cellular membranes into the cytoplasm to give a snapshot of intracellular chemical processes and metabolic flux distribution without causing significant damage. When coupled to automated microfluidics or LoC devices and deep machine learning, SERS would permit in/off/online platform to monitor therapeutic drug activity and patients' response to new drugs in real-time. However, disease diagnosis by SERS should be validated carefully and comprehensively, which may include confirmatory inputs from techniques presented in Table 1. This is aimed to avoid costly and risky unpredictable analytics like the blood testing system which led to the 'Theranos scandal', perhaps the biggest science saga of the 21st century to date. It is clearly evident that theranostics-SERS interface along with MVA will potentially revolutionise patient care, AMR biochemistry and drug discovery by expanding on the diagnostics and therapeutics toolbox for clinicians in the foreseeable future. We are hopeful this review will contribute to the ongoing efforts to translate vibrational spectroscopy to the clinic, spearheaded by the international society for clinical spectroscopy (CLIRSPEC) [160].

Table 1. A summary of different types of enhanced Raman scattering techniques commonly used in disease diagnostics.

Enhanced Raman Techniques	Brief Description
Resonance Raman (RR) scattering	RR occurs when the incident frequency excites electronic energy (EE) states of specific molecules; e.g., aromatic chromophores, and this aids the detection of pathogens [161]. If the EE level is excited by laser frequency in the ultraviolet (UV) region, the technique is UVRR, and can be susceptible to photodissociation [162].
Spatially offset Raman spectroscopy (SORS)	SORS collects distinctive chemical information and images from deep subsurfaces (including analytes in opaque containers) of a sample. SORS spectral signals are recorded when backscattered Raman photons are collected at points spatially offset (Δx) from the point of illumination (x). Negligible photodissociation, allowing for noninvasive deep medical diagnostics [163].
Surface-enhanced spatially offset Raman spectroscopy (SESORS)	SORS combined with NPs that enable SERS: that is to say subsurface information is measured from molecules in the vicinity of or chemically bonded to SERS substrates. Negligible fluorescence and excellent background contrast, specificity and sensitivity with improved detection limit for various disease markers [164,165].
Surface-enhanced spatially offset resonance Raman spectroscopy (SESORRS)	A variant of SESORS where incident frequency matches the EE of molecules near SERS-active substrates. SESORRS increases spectral signals further by orders of magnitude to provide extra biochemical selectivity and sensitivity, theoretically better than SESORS, as demonstrated by Fay et al. for breast cancer detection [166].
Tip-enhanced Raman spectroscopy (TERS)	Similar to the SERS phenomenon, but here a single SERS-active AFM probe whose sharp pointed apex (tip) is covered in NPs and scans through biomolecules on a sample surface, resulting in highly confined plasmonic enhancement (electrostatic lightning rod and SPR effects). Improves lateral spatial resolution to as low as 10 nm, about the diameter of the tip probe. Achieves single molecule detection and discrimination of bacterial pathogens [167,168].
Stimulated Raman scattering (SRS)	Two lasers provide a pump (ω_p) (similar to conventional Raman) and Stokes (ω_s) beam frequencies that intersect at the sample surface. The energy difference ($\Delta\omega = \omega_p - \omega_s$) between the beams matches the frequency (Ω_{vib}) of molecular bond vibrations, leading to larger scattering cross-section as a consequence of stimulated Raman excitation. No nonresonance background [169], making SRS ideal for in vivo medical imaging to improve disease diagnostics [170].
Coherent anti-Stokes Raman scattering (CARS)	Like SRS, CARS employs two lasers of frequencies ω_p and ω_s . When molecular bonds whose Ω_{vib} coincide with $\Delta\omega$ (as in SRS), anti-Stokes (<i>as</i>) lines are produced at frequency $\omega_{as} = 2\omega_p - \omega_s$. Thus, analytes are excited twice, from the ground to first and second excited states before relaxing back to the ground state. Though prone to nonresonance background effects which may limit the quantification of target analytes [171], CARS is effectively applied for disease detection including differential diagnostics of cancers [172].

Author Contributions: Conceptualisation, M.C. and R.G.; Writing—Original Draft Preparation, M.C.; Writing—Review & Editing, M.C., H.M., D.I.E. and R.G.; Supervision, R.G.

Funding: This research project was funded by the Commonwealth Scholarship Commission (CS) UK grant number ZMCA-2016-152 for M.C. and the UK Biotechnology and Biological Sciences Research Council (BBSRC) grant number BB/L014823/1 for R.G.

Conflicts of Interest: The authors declare no conflict of interest.

References

1. Trivedi, D.K.; Hollywood, K.A.; Goodacre, R. Metabolomics for the masses: The future of metabolomics in a personalized world. *New Horiz. Transl. Med.* **2017**, *3*, 294–305. [[CrossRef](#)] [[PubMed](#)]
2. Ellis, D.I.; Dunn, W.B.; Griffin, J.L.; Allwood, J.W.; Goodacre, R. Metabolic fingerprinting as a diagnostic tool. *Pharmacogenomics* **2007**, *8*, 1243–1266. [[CrossRef](#)] [[PubMed](#)]
3. Atkinson, A.J.; Colburn, W.A.; DeGruttola, V.G.; DeMets, D.L.; Downing, G.J.; Hoth, D.F.; Oates, J.A.; Peck, C.C.; Schooley, R.T.; Spilker, B.A.; et al. Biomarkers and surrogate endpoints: Preferred definitions and conceptual framework. *Clin. Pharmacol. Ther.* **2001**, *69*, 89–95.
4. Wheelock, C.E.; Goss, V.M.; Balgoma, D.; Nicholas, B.; Brandsma, J.; Skipp, P.J.; Snowden, S.; Burg, D.; D'Amico, A.; Horvath, I.; et al. Application of 'omics technologies to biomarker discovery in inflammatory lung diseases. *Eur. Respir. J.* **2013**, *42*, 802–825. [[CrossRef](#)] [[PubMed](#)]
5. Luo, P.; Yin, P.Y.; Hua, R.; Tan, Y.X.; Li, Z.F.; Qiu, G.K.; Yin, Z.Y.; Xie, X.W.; Wang, X.M.; Chen, W.B.; et al. A large-scale, multicenter serum metabolite biomarker identification study for the early detection of hepatocellular carcinoma. *Hepatology* **2018**, *67*, 662–675. [[CrossRef](#)]
6. Zhang, A.H.; Sun, H.; Wang, P.; Han, Y.; Wang, X.J. Modern analytical techniques in metabolomics analysis. *Analyst* **2012**, *137*, 293–300. [[CrossRef](#)]
7. Kitteringham, N.R.; Jenkins, R.E.; Lane, C.S.; Elliott, V.L.; Park, B.K. Multiple reaction monitoring for quantitative biomarker analysis in proteomics and metabolomics. *J. Chromatogr. B* **2009**, *877*, 1229–1239. [[CrossRef](#)]
8. Ayalew, M.; Le-Niculescu, H.; Levey, D.F.; Jain, N.; Changala, B.; Patel, S.D.; Winiger, E.; Breier, A.; Shekhar, A.; Amdur, R.; et al. Convergent functional genomics of schizophrenia: From comprehensive understanding to genetic risk prediction. *Mol. Psychiatry* **2012**, *17*, 887–905. [[CrossRef](#)]
9. Dunn, W.B.; Broadhurst, D.I.; Atherton, H.J.; Goodacre, R.; Griffin, J.L. Systems level studies of mammalian metabolomes: The roles of mass spectrometry and nuclear magnetic resonance spectroscopy. *Chem. Soc. Rev.* **2011**, *40*, 387–426. [[CrossRef](#)]
10. Goodacre, R.; Graham, D.; Faulds, K. Recent developments in quantitative SERS: Moving towards absolute quantification. *TrAC Trends Anal. Chem.* **2018**, *102*, 359–368. [[CrossRef](#)]
11. Levine, R.J.; Lam, C.; Qian, C.; Yu, K.F.; Maynard, S.E.; Sachs, B.P.; Sibai, B.M.; Epstein, F.H.; Romero, R.; Thadhani, R.; et al. Soluble endoglin and other circulating antiangiogenic factors in preeclampsia. *N. Engl. J. Med.* **2006**, *355*, 992–1005. [[CrossRef](#)]
12. Berger, A.G.; Restaino, S.M.; White, I.M. Vertical-flow paper SERS system for therapeutic drug monitoring of flucytosine in serum. *Anal. Chim. Acta* **2017**, *949*, 59–66. [[CrossRef](#)]
13. Graham, D.; Moskovits, M.; Tian, Z.Q. SERS—Facts, figures and the future. *Chem. Soc. Rev.* **2017**, *46*, 3864–3865. [[CrossRef](#)]
14. Tempero, M.A.; Malafa, M.P.; Al-Hawary, M.; Asbun, H.; Bain, A.; Behrman, S.W.; Benson, A.B.; Binder, E.; Cardin, D.B.; Cha, C.; et al. Pancreatic adenocarcinoma, version 2.2017, NCCN clinical practice guidelines in oncology. *J. Natl. Compr. Cancer Netw.* **2017**, *15*, 1028–1061. [[CrossRef](#)]
15. Tang, H.B.; Meng, G.W.; Huang, Q.; Zhang, Z.; Huang, Z.L.; Zhu, C.H. Arrays of cone-shaped ZnO nanorods decorated with Ag nanoparticles as 3D surface-enhanced Raman scattering substrates for rapid detection of trace polychlorinated biphenyls. *Adv. Funct. Mater.* **2012**, *22*, 218–224. [[CrossRef](#)]
16. Makam, P.; Shilpa, R.; Kandjani, A.E.; Periasamy, S.R.; Sabri, Y.M.; Madhu, C.; Bhargava, S.K.; Govindaraju, T. SERS and fluorescence-based ultrasensitive detection of mercury in water. *Biosens. Bioelectron.* **2018**, *100*, 556–564. [[CrossRef](#)]
17. Zhou, H.B.; Yang, D.T.; Ivleva, N.P.; Mircescu, N.E.; Schubert, S.; Niessner, R.; Wieser, A.; Haisch, C. Label-free in situ discrimination of live and dead bacteria by surface-enhanced Raman scattering. *Anal. Chem.* **2015**, *87*, 6553–6561. [[CrossRef](#)]

18. Galvan, D.D.; Yu, Q.M. Surface-enhanced Raman scattering for rapid detection and characterization of antibiotic-resistant bacteria. *Adv. Healthc. Mater.* **2018**, *7*, 1701335. [[CrossRef](#)]
19. Liu, B.; Zhou, P.; Liu, X.M.; Sun, X.; Li, H.; Lin, M.S. Detection of pesticides in fruits by surface-enhanced Raman spectroscopy coupled with gold nanostructures. *Food Bioprocess Technol.* **2013**, *6*, 710–718. [[CrossRef](#)]
20. Lin, M.; He, L.; Awika, J.; Yang, L.; Ledoux, D.R.; Li, H.; Mustapha, A. Detection of melamine in gluten, chicken feed, and processed foods using surface-enhanced Raman spectroscopy and HPLC. *J. Food Sci.* **2008**, *73*, T129–T134. [[CrossRef](#)]
21. Subaihi, A.; Almanqur, L.; Muhamadali, H.; AlMasoud, N.; Ellis, D.I.; Trivedi, D.K.; Hollywood, K.A.; Xu, Y.; Goodacre, R. Rapid, accurate, and quantitative detection of propranolol in multiple human biofluids via surface-enhanced Raman scattering. *Anal. Chem.* **2016**, *88*, 10884–10892. [[CrossRef](#)]
22. Tackman, E.C.; Trujillo, M.J.; Lockwood, T.L.E.; Merga, G.; Lieberman, M.; Camden, J.P. Identification of substandard and falsified antimalarial pharmaceuticals chloroquine, doxycycline, and primaquine using surface-enhanced Raman scattering. *Anal. Methods* **2018**, *10*, 4718–4722. [[CrossRef](#)]
23. Jamieson, L.E.; Asiala, S.M.; Gracie, K.; Faulds, K.; Graham, D. Bioanalytical measurements enabled by surface-enhanced Raman scattering (SERS) probes. *Annu. Rev. Anal. Chem.* **2017**, *10*, 415–437. [[CrossRef](#)] [[PubMed](#)]
24. Laing, S.; Gracie, K.; Faulds, K. Multiplex in vitro detection using SERS. *Chem. Soc. Rev.* **2016**, *45*, 1901–1918. [[CrossRef](#)] [[PubMed](#)]
25. Feng, S.Y.; Chen, R.; Lin, J.Q.; Pan, J.J.; Chen, G.N.; Li, Y.Z.; Cheng, M.; Huang, Z.F.; Chen, J.; Zeng, H.S. Nasopharyngeal cancer detection based on blood plasma surface-enhanced Raman spectroscopy and multivariate analysis. *Biosens. Bioelectron.* **2010**, *25*, 2414–2419. [[CrossRef](#)] [[PubMed](#)]
26. Shao, L.T.; Zhang, A.Y.; Rong, Z.; Wang, C.W.; Jia, X.F.; Zhang, K.H.; Xiao, R.; Wang, S.Q. Fast and non-invasive serum detection technology based on surface-enhanced Raman spectroscopy and multivariate statistical analysis for liver disease. *Nanomed. Nanotechnol. Biol. Med.* **2018**, *14*, 451–459. [[CrossRef](#)] [[PubMed](#)]
27. Yang, S.K.; Dai, X.M.; Stogin, B.B.; Wong, T.S. Ultrasensitive surface-enhanced Raman scattering detection in common fluids. *Proc. Natl. Acad. Sci. USA* **2016**, *113*, 268–273. [[CrossRef](#)] [[PubMed](#)]
28. Subaihi, A.; Trivedi, D.K.; Hollywood, K.A.; Bluett, J.; Xu, Y.; Muhamadali, H.; Ellis, D.I.; Goodacre, R. Quantitative online liquid chromatography surface-enhanced Raman scattering (LC-SERS) of methotrexate and its major metabolites. *Anal. Chem.* **2017**, *89*, 6702–6709. [[CrossRef](#)] [[PubMed](#)]
29. Laing, S.; Jamieson, L.E.; Faulds, K.; Graham, D. Surface-enhanced Raman spectroscopy for in vivo biosensing. *Nat. Rev. Chem.* **2017**, *1*, 0060. [[CrossRef](#)]
30. Gracie, K.; Lindsay, D.; Graham, D.; Faulds, K. Bacterial meningitis pathogens identified in clinical samples using a SERS DNA detection assay. *Anal. Methods* **2015**, *7*, 1269–1272. [[CrossRef](#)]
31. Gracie, K.; Correa, E.; Mabbott, S.; Dougan, J.A.; Graham, D.; Goodacre, R.; Faulds, K. Simultaneous detection and quantification of three bacterial meningitis pathogens by SERS. *Chem. Sci.* **2014**, *5*, 1030–1040. [[CrossRef](#)]
32. Smekal, A. On the quantum theory of dispersal and dispersion. *Z. Phys.* **1925**, *32*, 241–244. [[CrossRef](#)]
33. Raman, C.V.; Krishnan, K.S. A new type of secondary radiation. *Nature* **1928**, *121*, 501–502. [[CrossRef](#)]
34. Ellis, D.I.; Goodacre, R. Metabolic fingerprinting in disease diagnosis: Biomedical applications of infrared and Raman spectroscopy. *Analyst* **2006**, *131*, 875–885. [[CrossRef](#)]
35. Fleischmann, M.; Hendra, P.J.; McQuillan, A.J. Raman spectra of pyridine adsorbed at a silver electrode. *Chem. Phys. Lett.* **1974**, *26*, 163–166. [[CrossRef](#)]
36. Jeanmaire, D.L.; Vanduyne, R.P. Surface Raman spectroelectrochemistry. 1. Heterocyclic, aromatic, and aliphatic-amines adsorbed on anodized silver electrode. *J. Electroanal. Chem.* **1977**, *84*, 1–20. [[CrossRef](#)]
37. Albrecht, M.G.; Creighton, J.A. Anomalously intense Raman spectra of pyridine at a silver electrode. *J. Am. Chem. Soc.* **1977**, *99*, 5215–5217. [[CrossRef](#)]
38. Sharma, B.; Frontiera, R.R.; Henry, A.I.; Ringe, E.; Van Duyne, R.P. SERS: Materials, applications, and the future. *Mater. Today* **2012**, *15*, 16–25. [[CrossRef](#)]
39. Graham, D.; Goodacre, R.; Arnolds, H.; Masson, J.F.; Schatz, G.; Baumberg, J.; Kim, D.H.; Aizpurua, J.; Lum, W.; Silvestri, A.; et al. Theory of SERS enhancement: General discussion. *Faraday Discuss.* **2017**, *205*, 173–211. [[CrossRef](#)]
40. Moskovits, M.; Suh, J.S. Surface selection-rules for surface-enhanced Raman spectroscopy—Calculations and application to the surface-enhanced Raman-spectrum of phthalazine on silver. *J. Phys. Chem.* **1984**, *88*, 5526–5530. [[CrossRef](#)]

41. Willets, K.A.; Van Duyne, R.P. Localized surface plasmon resonance spectroscopy and sensing. *Annu. Rev. Phys. Chem.* **2007**, *58*, 267–297. [[CrossRef](#)]
42. Stiles, P.L.; Dieringer, J.A.; Shah, N.C.; Van Duyne, R.R. Surface-enhanced Raman spectroscopy. *Annu. Rev. Anal. Chem.* **2008**, *1*, 601–626. [[CrossRef](#)]
43. Schlucker, S. Surface-enhanced Raman spectroscopy: Concepts and chemical applications. *Angew. Chem.-Int. Ed.* **2014**, *53*, 4756–4795. [[CrossRef](#)]
44. Qian, X.M.; Nie, S.M. Single-molecule and single-nanoparticle SERS: From fundamental mechanisms to biomedical applications. *Chem. Soc. Rev.* **2008**, *37*, 912–920. [[CrossRef](#)]
45. Kneipp, K.; Wang, Y.; Kneipp, H.; Perelman, L.T.; Itzkan, I.; Dasari, R.; Feld, M.S. Single molecule detection using surface-enhanced Raman scattering (SERS). *Phys. Rev. Lett.* **1997**, *78*, 1667–1670. [[CrossRef](#)]
46. Fisk, H.; Westley, C.; Turner, N.J.; Goodacre, R. Achieving optimal SERS through enhanced experimental design. *J. Raman Spectrosc.* **2016**, *47*, 59–66. [[CrossRef](#)]
47. Zong, C.; Xu, M.X.; Xu, L.J.; Wei, T.; Ma, X.; Zheng, X.S.; Hu, R.; Ren, B. Surface-enhanced Raman spectroscopy for bioanalysis: Reliability and challenges. *Chem. Rev.* **2018**, *118*, 4946–4980. [[CrossRef](#)]
48. Wang, Y.; Ruan, Q.Y.; Lei, Z.C.; Ling, S.C.; Zhu, Z.; Zhou, L.J.; Yang, C.Y. Highly sensitive and automated surface-enhanced Raman scattering-based immunoassay for H5N1 detection with digital microfluidics. *Anal. Chem.* **2018**, *90*, 5224–5231. [[CrossRef](#)]
49. Cialla-May, D.; Zheng, X.S.; Weber, K.; Popp, J. Recent progress in surface-enhanced Raman spectroscopy for biological and biomedical applications: From cells to clinics. *Chem. Soc. Rev.* **2017**, *46*, 3945–3961. [[CrossRef](#)]
50. Howes, P.D.; Chandrawati, R.; Stevens, M.M. Colloidal nanoparticles as advanced biological sensors. *Science* **2014**, *346*, 1247390. [[CrossRef](#)]
51. Austin, L.A.; Mackey, M.A.; Dreaden, E.C.; El-Sayed, M.A. The optical, photothermal, and facile surface chemical properties of gold and silver nanoparticles in biodiagnostics, therapy, and drug delivery. *Arch. Toxicol.* **2014**, *88*, 1391–1417. [[CrossRef](#)] [[PubMed](#)]
52. Lombardi, J.R.; Birke, R.L. A unified approach to surface-enhanced Raman spectroscopy. *J. Phys. Chem. C* **2008**, *112*, 5605–5617. [[CrossRef](#)]
53. Xu, L.J.; Lei, Z.C.; Li, J.X.; Zong, C.; Yang, C.J.; Ren, B. Label-free surface-enhanced Raman spectroscopy detection of DNA with single-base sensitivity. *J. Am. Chem. Soc.* **2015**, *137*, 5149–5154. [[CrossRef](#)] [[PubMed](#)]
54. Bonifacio, A.; Cervo, S.; Sergio, V. Label-free surface-enhanced Raman spectroscopy of biofluids: Fundamental aspects and diagnostic applications. *Anal. Bioanal. Chem.* **2015**, *407*, 8265–8277. [[CrossRef](#)] [[PubMed](#)]
55. Wold, S.; Esbensen, K.; Geladi, P. Principal component analysis. *Chemom. Intell. Lab. Syst.* **1987**, *2*, 37–52. [[CrossRef](#)]
56. Granato, D.; Santos, J.S.; Escher, G.B.; Ferreira, B.L.; Maggio, R.M. Use of principal component analysis (PCA) and hierarchical cluster analysis (HCA) for multivariate association between bioactive compounds and functional properties in foods: A critical perspective. *Trends Food Sci. Technol.* **2018**, *72*, 83–90. [[CrossRef](#)]
57. Muhamadali, H.; Chisanga, M.; Subaihi, A.; Goodacre, R. Combining Raman and FT-IR spectroscopy with quantitative isotopic labeling for differentiation of *E. coli* cells at community and single cell levels. *Anal. Chem.* **2015**, *87*, 4578–4586. [[CrossRef](#)]
58. Wold, S.; Sjostrom, M.; Eriksson, L. Pls-regression: A basic tool of chemometrics. *Chemom. Intell. Lab. Syst.* **2001**, *58*, 109–130. [[CrossRef](#)]
59. Gromski, P.S.; Muhamadali, H.; Ellis, D.I.; Xu, Y.; Correa, E.; Turner, M.L.; Goodacre, R. A tutorial review: Metabolomics and partial least squares-discriminant analysis—A marriage of convenience or a shotgun wedding. *Anal. Chim. Acta* **2015**, *879*, 10–23. [[CrossRef](#)]
60. Mazivila, S.J.; Olivieri, A.C. Chemometrics coupled to vibrational spectroscopy and spectroscopic imaging for the analysis of solid-phase pharmaceutical products: A brief review on non-destructive analytical methods. *TrAC-Trends Anal. Chem.* **2018**, *108*, 74–87. [[CrossRef](#)]
61. Shinzawa, H.; Awa, K.; Kanematsu, W.; Ozaki, Y. Multivariate data analysis for Raman spectroscopic imaging. *J. Raman Spectrosc.* **2009**, *40*, 1720–1725. [[CrossRef](#)]
62. Ellis, D.I.; Brewster, V.L.; Dunn, W.B.; Allwood, J.W.; Golovanov, A.P.; Goodacre, R. Fingerprinting food: Current technologies for the detection of food adulteration and contamination. *Chem. Soc. Rev.* **2012**, *41*, 5706–5727. [[CrossRef](#)]
63. Schmidhuber, J. Deep learning in neural networks: An overview. *Neural Netw.* **2015**, *61*, 85–117. [[CrossRef](#)]

64. Rumelhart, D.E.; McClelland, J.L.; Group, P.R. *Parallel Distributed Processing, Experiments in the Microstructure of Cognition*; MIT Press: Cambridge, MA, USA, 1986; Volumes 1–2.
65. Shi, H.Y.; Wang, H.Y.; Meng, X.Y.; Chen, R.Z.; Zhang, Y.S.; Su, Y.Y.; He, Y. Setting up a surface-enhanced Raman scattering database for artificial-intelligence-based label-free discrimination of tumor suppressor genes. *Anal. Chem.* **2018**, *90*, 14216–14221. [[CrossRef](#)]
66. Krauss, S.D.; Roy, R.; Yosef, H.K.; Lechtonen, T.; El-Mashtoly, S.F.; Gerwert, K.; Mosig, A. Hierarchical deep convolutional neural networks combine spectral and spatial information for highly accurate raman-microscopy-based cytopathology. *J. Biophotonics* **2018**, *11*, e201800022. [[CrossRef](#)]
67. Broadhurst, D.I.; Kell, D.B. Statistical strategies for avoiding false discoveries in metabolomics and related experiments. *Metabolomics* **2006**, *2*, 171–196. [[CrossRef](#)]
68. Lin, D.; Feng, S.Y.; Pan, J.J.; Chen, Y.P.; Lin, J.Q.; Chen, G.N.; Xie, S.S.; Zeng, H.S.; Chen, R. Colorectal cancer detection by gold nanoparticle based surface-enhanced Raman spectroscopy of blood serum and statistical analysis. *Opt. Express* **2011**, *19*, 13565–13577. [[CrossRef](#)]
69. Chen, Y.P.; Chen, G.; Feng, S.Y.; Pan, J.J.; Zheng, X.W.; Su, Y.; Chen, Y.; Huang, Z.F.; Lin, X.Q.; Lan, F.H.; et al. Label-free serum ribonucleic acid analysis for colorectal cancer detection by surface-enhanced Raman spectroscopy and multivariate analysis. *J. Biomed. Opt.* **2012**, *17*, 067003. [[CrossRef](#)]
70. Yu, Y.; Lin, Y.T.; Xu, C.X.; Lin, K.C.; Ye, Q.; Wang, X.Y.; Xie, S.S.; Chen, R.; Lin, J.Q. Label-free detection of nasopharyngeal and liver cancer using surface-enhanced Raman spectroscopy and partial least squares combined with support vector machine. *Biomed. Opt. Express* **2018**, *9*, 6053–6066. [[CrossRef](#)]
71. Carmicheal, J.; Hayashi, C.; Huang, X.; Liu, L.; Lu, Y.; Krasnoslobodtsev, A.; Lushnikov, A.; Kshirsagar, P.G.; Patel, A.; Jain, M.; et al. Label-free characterization of exosome via surface-enhanced Raman spectroscopy for the early detection of pancreatic cancer. *Nanomed. Nanotechnol. Biol. Med.* **2019**, *16*, 88–96. [[CrossRef](#)]
72. Jarvis, R.M.; Goodacre, R. Discrimination of bacteria using surface-enhanced Raman spectroscopy. *Anal. Chem.* **2004**, *76*, 40–47. [[CrossRef](#)]
73. Kearns, H.; Goodacre, R.; Jamieson, L.E.; Graham, D.; Faulds, K. SERS detection of multiple antimicrobial-resistant pathogens using nanosensors. *Anal. Chem.* **2017**, *89*, 12666–12673. [[CrossRef](#)]
74. Lu, Y.D.; Lin, Y.S.; Zheng, Z.C.; Tang, X.Q.; Lin, J.Y.; Liu, X.J.; Liu, M.M.; Chen, G.N.; Qiu, S.F.; Zhou, T.; et al. Label free hepatitis B detection based on serum derivative surface-enhanced Raman spectroscopy combined with multivariate analysis. *Biomed. Opt. Express* **2018**, *9*, 4755–4766. [[CrossRef](#)]
75. Hidi, I.J.; Jahn, M.; Weber, K.; Bocklitz, T.; Pletz, M.W.; Cialla-May, D.; Popp, J. Lab-on-a-chip-surface-enhanced Raman scattering combined with the standard addition method: Toward the quantification of nitroxoline in spiked human urine samples. *Anal. Chem.* **2016**, *88*, 9173–9180. [[CrossRef](#)]
76. Alharbi, O.; Xu, Y.; Goodacre, R. Simultaneous multiplexed quantification of caffeine and its major metabolites theobromine and paraxanthine using surface-enhanced Raman scattering. *Anal. Bioanal. Chem.* **2015**, *407*, 8253–8261. [[CrossRef](#)]
77. Deng, B.E.; Luo, X.; Zhang, M.; Ye, L.M.; Chen, Y. Quantitative detection of acyclovir by surface-enhanced Raman spectroscopy using a portable Raman spectrometer coupled with multivariate data analysis. *Colloid Surf. B Biointerfaces* **2019**, *173*, 286–294. [[CrossRef](#)]
78. Fitzmaurice, C.; Allen, C.; Barber, R.M.; Barregard, L.; Bhutta, Z.A.; Brenner, H.; Dicker, D.J.; Chimed-Orchir, O.; Dandona, R.; Dandona, L.; et al. Global, regional, and national cancer incidence, mortality, years of life lost, years lived with disability, and disability-adjusted life-years for 32 cancer groups, 1990 to 2015 a systematic analysis for the global burden of disease study. *JAMA Oncol.* **2017**, *3*, 524–548.
79. World Health Organisation. Available online: <https://www.Who.Int/en/news-room/fact-sheets/detail/cancer> (accessed on 12 December 2018).
80. Chikkaveeraiah, B.V.; Bhirde, A.A.; Morgan, N.Y.; Eden, H.S.; Chen, X.Y. Electrochemical immunosensors for detection of cancer protein biomarkers. *ACS Nano* **2012**, *6*, 6546–6561. [[CrossRef](#)]
81. Wu, L.; Qu, X.G. Cancer biomarker detection: Recent achievements and challenges. *Chem. Soc. Rev.* **2015**, *44*, 2963–2997. [[CrossRef](#)]
82. Wang, W.S.; Lin, J.K.; Lin, T.C.; Chiou, T.J.; Liu, J.H.; Yen, C.C.; Chen, W.S.; Jiang, J.K.; Yang, S.H.; Wang, H.S.; et al. EIA versus RIA in detecting carcinoembryonic antigen level of patients with metastatic colorectal cancer. *Hepato-Gastroenterol.* **2004**, *51*, 136–141.

83. Lim, S.; Janzer, A.; Becker, A.; Zimmer, A.; Schule, R.; Buettner, R.; Kirfel, J. Lysine-specific demethylase 1 (LSD1) is highly expressed in ER-negative breast cancers and a biomarker predicting aggressive biology. *Carcinogenesis* **2010**, *31*, 512–520. [[CrossRef](#)] [[PubMed](#)]
84. Kim, S.E.; Kim, Y.J.; Song, S.; Lee, K.N.; Seong, W.K. A simple electrochemical immunosensor platform for detection of apolipoprotein A1 (Apo-A1) as a bladder cancer biomarker in urine. *Sens. Actuator B Chem.* **2019**, *278*, 103–109. [[CrossRef](#)]
85. Ambrosi, A.; Airo, F.; Merkoci, A. Enhanced gold nanoparticle based ELISA for a breast cancer biomarker. *Anal. Chem.* **2010**, *82*, 1151–1156. [[CrossRef](#)]
86. Fitzgerald, S.; O'Reilly, J.A.; Wilson, E.; Joyce, A.; Farrell, R.; Kenny, D.; Kay, E.W.; Fitzgerald, J.; Byrne, B.; Kijanka, G.S.; et al. Measurement of the IgM and IgG autoantibody immune responses in human serum has high predictive value for the presence of colorectal cancer. *Clin. Colorectal Cancer* **2018**, in press. [[CrossRef](#)] [[PubMed](#)]
87. Zhu, Y.D.; Peng, J.; Jiang, L.P.; Zhu, J.J. Fluorescent immunosensor based on CuS nanoparticles for sensitive detection of cancer biomarker. *Analyst* **2014**, *139*, 649–655. [[CrossRef](#)]
88. Zhou, Y.F.; Huang, X.L.; Xiong, S.C.; Li, X.M.; Zhan, S.N.; Zeng, L.F.; Xiong, Y.H. Dual-mode fluorescent and colorimetric immunoassay for the ultrasensitive detection of alpha-fetoprotein in serum samples. *Anal. Chim. Acta* **2018**, *1038*, 112–119. [[CrossRef](#)] [[PubMed](#)]
89. Chon, H.; Lee, S.; Son, S.W.; Oh, C.H.; Choo, J. Highly sensitive immunoassay of lung cancer marker carcinoembryonic antigen using surface-enhanced Raman scattering of hollow gold nanospheres. *Anal. Chem.* **2009**, *81*, 3029–3034. [[CrossRef](#)] [[PubMed](#)]
90. Wang, G.F.; Lipert, R.J.; Jain, M.; Kaur, S.; Chakraborty, S.; Torres, M.P.; Batra, S.K.; Brand, R.E.; Porter, M.D. Detection of the potential pancreatic cancer marker MUC4 in serum using surface-enhanced Raman scattering. *Anal. Chem.* **2011**, *83*, 2554–2561. [[CrossRef](#)]
91. Li, J.R.; Wang, J.; Grewal, Y.S.; Howard, C.B.; Raftery, L.J.; Mahler, S.; Wang, Y.L.; Trau, M. Multiplexed SERS detection of soluble cancer protein biomarkers with gold-silver alloy nanoboxes and nanoyeast single-chain variable fragments. *Anal. Chem.* **2018**, *90*, 10377–10384. [[CrossRef](#)]
92. Nguyen, A.H.; Lee, J.; Choi, H.I.; Kwak, H.S.; Sim, S.J. Fabrication of plasmon length-based surface-enhanced Raman scattering for multiplex detection on microfluidic device. *Biosens. Bioelectron.* **2015**, *70*, 358–365. [[CrossRef](#)]
93. Ma, H.; Sun, X.Y.; Chen, L.; Han, X.X.; Zhao, B.; Lu, H.; He, C.Y. Antibody-free discrimination of protein biomarkers in human serum based on surface-enhanced Raman spectroscopy. *Anal. Chem.* **2018**, *90*, 12342–12346. [[CrossRef](#)]
94. Qian, X.M.; Peng, X.H.; Ansari, D.O.; Yin-Goen, Q.; Chen, G.Z.; Shin, D.M.; Yang, L.; Young, A.N.; Wang, M.D.; Nie, S.M. *In vivo* tumor targeting and spectroscopic detection with surface-enhanced Raman nanoparticle tags. *Nat. Biotechnol.* **2008**, *26*, 83–90. [[CrossRef](#)]
95. Faulds, K.; McKenzie, F.; Smith, W.E.; Graham, D. Quantitative simultaneous multianalyte detection of DNA by dual-wavelength surface-enhanced resonance Raman scattering. *Angew. Chem.-Int. Ed.* **2007**, *46*, 1829–1831. [[CrossRef](#)]
96. Cheng, Z.; Choi, N.; Wang, R.; Lee, S.; Moon, K.C.; Yoon, S.Y.; Chen, L.X.; Choo, J. Simultaneous detection of dual prostate specific antigens using surface-enhanced Raman scattering-based immunoassay for accurate diagnosis of prostate cancer. *ACS Nano* **2017**, *11*, 4926–4933. [[CrossRef](#)]
97. Banaei, N.; Foley, A.; Houghton, J.M.; Sun, Y.B.; Kim, B. Multiplex detection of pancreatic cancer biomarkers using a SERS-based immunoassay. *Nanotechnology* **2017**, *28*, 455101. [[CrossRef](#)]
98. Hwang, H.; Chon, H.; Choo, J.; Park, J.K. Optoelectrofluidic sandwich immunoassays for detection of human tumor marker using surface-enhanced Raman scattering. *Anal. Chem.* **2010**, *82*, 7603–7610. [[CrossRef](#)]
99. Neng, J.; Harpster, M.H.; Zhang, H.; Mecham, J.O.; Wilson, W.C.; Johnson, P.A. A versatile SERS-based immunoassay for immunoglobulin detection using antigen-coated gold nanoparticles and malachite green-conjugated protein A/G. *Biosens. Bioelectron.* **2010**, *26*, 1009–1015. [[CrossRef](#)]
100. Gao, R.K.; Cheng, Z.Y.; Demello, A.J.; Choo, J. Wash-free magnetic immunoassay of the PSA cancer marker using SERS and droplet microfluidics. *Lab Chip* **2016**, *16*, 1022–1029. [[CrossRef](#)]
101. Perozziello, G.; Candeloro, P.; Gentile, F.; Nicastrì, A.; Perri, A.; Coluccio, M.L.; Adamo, A.; Pardeo, F.; Catalano, R.; Parrotta, E.; et al. Microfluidics & nanotechnology: Towards fully integrated analytical devices for the detection of cancer biomarkers. *RSC Adv.* **2014**, *4*, 55590–55598.

102. Wee, E.J.H.; Wang, Y.L.; Tsao, S.C.H.; Trau, M. Simple, sensitive and accurate multiplex detection of clinically important melanoma DNA mutations in circulating tumour DNA with SERS nanotags. *Theranostics* **2016**, *6*, 1506–1513. [CrossRef]
103. Goodacre, R. Metabolomics of a superorganism. *J. Nutr.* **2007**, *137*, 259S–266S. [CrossRef]
104. World Health Organisation Global Statistics. p. 30. Available online: <http://apps.who.int/iris/bitstream/handle/10665/255336/9789241565486-eng.Pdf?Sequence=1> (accessed on 3 January 2018).
105. Ellis, D.I.; Muhamadali, H.; Chisanga, M.; Goodacre, R. Omics methods for the detection of foodborne pathogens. *Encycl. Food Chem.* **2019**, *1*, 364–370.
106. World Health Organisation. Available online: <https://www.who.int/sustainable-development/housing/health-risks/waterborne-disease/en/> (accessed on 29 December 2018).
107. Food Consulting Strategically. Available online: <https://www.Focos-food.Com/campylobacter-on-the-rise-in-germany-every-second-chicken-in-germany-is-contaminated/> (accessed on 12 January 2019).
108. Lazcka, O.; Del Campo, F.J.; Munoz, F.X. Pathogen detection: A perspective of traditional methods and biosensors. *Biosens. Bioelectron.* **2007**, *22*, 1205–1217. [CrossRef] [PubMed]
109. Frieden, T.R.; Sterling, T.R.; Munsiff, S.S.; Watt, C.J.; Dye, C. Tuberculosis. *Lancet* **2003**, *362*, 887–899. [CrossRef]
110. Muhamadali, H.; Weaver, D.; Subaihi, A.; AlMasoud, N.; Trivedi, D.K.; Ellis, D.I.; Linton, D.; Goodacre, R. Chicken, beams, and *Campylobacter*: Rapid differentiation of foodborne bacteria via vibrational spectroscopy and MALDI-mass spectrometry. *Analyst* **2016**, *141*, 111–122. [CrossRef] [PubMed]
111. Santiago-Felipe, S.; Tortajada-Genaro, L.A.; Puchades, R.; Maquieira, A. Recombinase polymerase and enzyme-linked immunosorbent assay as a DNA amplification-detection strategy for food analysis. *Anal. Chim. Acta* **2014**, *811*, 81–87. [CrossRef]
112. Pang, B.; Zhao, C.; Li, L.; Song, X.L.; Xu, K.; Wang, J.; Liu, Y.S.; Fu, K.Y.; Bao, H.; Song, D.D.; et al. Development of a low-cost paper-based ELISA method for rapid *Escherichia coli* O157:H7 detection. *Anal. Biochem.* **2018**, *542*, 58–62. [CrossRef]
113. Catala, C.; Mir-Simon, B.; Feng, X.T.; Cardozo, C.; Pazos-Perez, N.; Pazos, E.; Gomez-de Pedro, S.; Guerrini, L.; Soriano, A.; Vila, J.; et al. Online SERS quantification of *Staphylococcus aureus* and the application to diagnostics in human fluids. *Adv. Mater. Technol.* **2016**, *1*, 1600163. [CrossRef]
114. Muhamadali, H.; Subaihi, A.; Mohammadtaheri, M.; Xu, Y.; Ellis, D.I.; Ramanathan, R.; Bansal, V.; Goodacre, R. Rapid, accurate, and comparative differentiation of clinically and industrially relevant microorganisms via multiple vibrational spectroscopic fingerprinting. *Analyst* **2016**, *141*, 5127–5136. [CrossRef]
115. Tien, N.; Lin, T.H.; Hung, Z.C.; Lin, H.S.; Wang, I.K.; Chen, H.C.; Chang, C.T. Diagnosis of bacterial pathogens in the urine of urinary-tract-infection patients using surface-enhanced Raman spectroscopy. *Molecules* **2018**, *23*, 3374. [CrossRef]
116. Shanmukh, S.; Jones, L.; Zhao, Y.P.; Driskell, J.D.; Tripp, R.A.; Dluhy, R.A. Identification and classification of respiratory syncytial virus (RSV) strains by surface-enhanced Raman spectroscopy and multivariate statistical techniques. *Anal. Bioanal. Chem.* **2008**, *390*, 1551–1555. [CrossRef]
117. Chen, Y.; Premasiri, W.R.; Ziegler, L.D. Surface-enhanced Raman spectroscopy of *Chlamydia trachomatis* and *Neisseria gonorrhoeae* for diagnostics, and extra-cellular metabolomics and biochemical monitoring. *Sci. Rep.* **2018**, *8*, 5163. [CrossRef]
118. Witkowska, E.; Jagielski, T.; Kaminska, A. Genus- and species-level identification of dermatophyte fungi by surface-enhanced Raman spectroscopy. *Spectrosc. Acta Part A Mol. Biomol. Spectr.* **2018**, *192*, 285–290. [CrossRef] [PubMed]
119. Chisanga, M.; Muhamadali, H.; Kimber, R.; Goodacre, R. Quantitative detection of isotopically enriched *E. coli* cells by SERS. *Faraday Discuss.* **2017**, *205*, 331–343. [CrossRef]
120. Efrima, S.; Zeiri, L. Understanding SERS of bacteria. *J. Raman Spectrosc.* **2009**, *40*, 277–288. [CrossRef]
121. Jarvis, R.M.; Brooker, A.; Goodacre, R. Surface-enhanced Raman spectroscopy for bacterial discrimination utilizing a scanning electron microscope with a Raman spectroscopy interface. *Anal. Chem.* **2004**, *76*, 5198–5202. [CrossRef] [PubMed]
122. Dina, N.E.; Gherman, A.M.R.; Chis, V.; Sarbu, C.; Wieser, A.; Bauer, D.; Haisch, C. Characterization of clinically relevant fungi via SERS fingerprinting assisted by novel chemometric models. *Anal. Chem.* **2018**, *90*, 2484–2492. [CrossRef]

123. Liu, C.Y.; Han, Y.Y.; Shih, P.H.; Lian, W.N.; Wang, H.H.; Lin, C.H.; Hsueh, P.R.; Wang, J.K.; Wang, Y.L. Rapid bacterial antibiotic susceptibility test based on simple surface-enhanced Raman spectroscopic biomarkers. *Sci. Rep.* **2016**, *6*, 23375. [CrossRef]
124. Berry, D.; Mader, E.; Lee, T.K.; Woebken, D.; Wang, Y.; Zhu, D.; Palatinszky, M.; Schintmeister, A.; Schmid, M.C.; Hanson, B.T.; et al. Tracking heavy water (D₂O) incorporation for identifying and sorting active microbial cells. *Proc. Natl. Acad. Sci. USA* **2015**, *112*, E194–E203. [CrossRef]
125. Wang, Y.; Song, Y.Z.; Tao, Y.F.; Muhamadali, H.; Goodacre, R.; Zhou, N.Y.; Preston, G.M.; Xu, J.; Huang, W.E. Reverse and multiple stable isotope probing to study bacterial metabolism and interactions at the single cell level. *Anal. Chem.* **2016**, *88*, 9443–9450. [CrossRef]
126. Leask, F. Renishaw diagnostics Announces CE Marking of RenDx Multiplex Assay System and Fungiplex Assay. SelectScience. 2015. Available online: <http://www.selectscience.net/industry-news/renishaw-diagnostics-announces-cemarking-of-rendx-multiplex-assay-system-andfungiplex-assay/?artID=38483> (accessed on 30 December 2018).
127. Neng, J.; Li, Y.N.; Driscoll, A.J.; Wilson, W.C.; Johnson, P.A. Detection of multiple pathogens in serum using silica-encapsulated nanotags in a surface-enhanced Raman scattering-based immunoassay. *J. Agric. Food Chem.* **2018**, *66*, 5707–5712. [CrossRef] [PubMed]
128. Sebba, D.; Lastovich, A.G.; Kuroda, M.; Fallows, E.; Johnson, J.; Ahouidi, A.; Honko, A.N.; Fu, H.; Nielson, R.; Carruthers, E.; et al. A point-of-care diagnostic for differentiating Ebola from endemic febrile diseases. *Sci. Transl. Med.* **2018**, *10*, eaat0944. [CrossRef] [PubMed]
129. Muhlig, A.; Bocklitz, T.; Labugger, I.; Dees, S.; Henk, S.; Richter, E.; Andres, S.; Merker, M.; Stockel, S.; Weber, K.; et al. LOC-SERS: A promising closed system for the identification of mycobacteria. *Anal. Chem.* **2016**, *88*, 7998–8004. [CrossRef]
130. Willner, M.R.; McMillan, K.S.; Graham, D.; Vikesland, P.J.; Zagnoni, M. Surface-enhanced Raman scattering based microfluidics for single-cell analysis. *Anal. Chem.* **2018**, *90*, 12004–12010. [CrossRef] [PubMed]
131. Patel, I.S.; Premasiri, W.R.; Moir, D.T.; Ziegler, L.D. Barcoding bacterial cells: A SERS-based methodology for pathogen identification. *J. Raman Spectrosc.* **2008**, *39*, 1660–1672. [CrossRef]
132. Shikha, S.; Salafi, T.; Cheng, J.T.; Zhang, Y. Versatile design and synthesis of nano-barcodes. *Chem. Soc. Rev.* **2017**, *46*, 7054–7093. [CrossRef]
133. Bos, L.D.; Sterk, P.J.; Fowler, S.J. Breathomics in the setting of asthma and chronic obstructive pulmonary disease. *J. Allergy Clin. Immunol.* **2016**, *138*, 970–976. [CrossRef] [PubMed]
134. Rattray, N.J.W.; Hamrang, Z.; Trivedi, D.K.; Goodacre, R.; Fowler, S.J. Taking your breath away: Metabolomics breathes life in to personalized medicine. *Trends Biotechnol.* **2014**, *32*, 538–548. [CrossRef] [PubMed]
135. Alonso, M.; Sanchez, J.M. Analytical challenges in breath analysis and its application to exposure monitoring. *TrAC-Trends Anal. Chem.* **2013**, *44*, 78–89. [CrossRef]
136. de Vries, R.; Dagelet, Y.W.F.; Spoor, P.; Snoey, E.; Jak, P.M.C.; Brinkman, P.; Dijkers, E.; Bootsma, S.K.; Elskamp, F.; de Jongh, F.H.C.; et al. Clinical and inflammatory phenotyping by breathomics in chronic airway diseases irrespective of the diagnostic label. *Eur. Resp. J.* **2018**, *51*, 1701817. [CrossRef]
137. Neerincx, A.H.; Vijverberg, S.J.H.; Bos, L.D.J.; Brinkman, P.; van der Schee, M.P.; de Vries, R.; Sterk, P.J.; Maitland-van der Zee, A.H. Breathomics from exhaled volatile organic compounds in pediatric asthma. *Pediatr. Pulmonol.* **2017**, *52*, 1616–1627. [CrossRef] [PubMed]
138. Aizpurua, J.; Arnolds, H.; Baumberg, J.; Bruzas, I.; Chikkaraddy, R.; Chisanga, M.; Dawson, P.; Deckert, V.; Delfino, I.; de Nijs, B.; et al. Ultrasensitive and towards single molecule SERS: General discussion. *Faraday Discuss.* **2017**, *205*, 291–330. [CrossRef] [PubMed]
139. Wong, C.L.; Dinish, U.S.; Buddharaju, K.D.; Schmidt, M.S.; Olivo, M. Surface-enhanced Raman scattering (SERS)-based volatile organic compounds (VOCs) detection using plasmonic bimetallic nanogap substrate. *Appl. Phys. A Mater. Sci. Process.* **2014**, *117*, 687–692. [CrossRef]
140. Wong, C.L.; Dinish, U.S.; Schmidt, M.S.; Olivo, M. Non-labeling multiplex surface-enhanced Raman scattering (SERS) detection of volatile organic compounds (VOCs). *Anal. Chim. Acta* **2014**, *844*, 54–60. [CrossRef] [PubMed]
141. Chen, Y.S.; Zhang, Y.X.; Pan, F.; Liu, J.; Wang, K.; Zhang, C.L.; Cheng, S.L.; Lu, L.G.; Zhang, W.; Zhang, Z.; et al. Breath analysis based on surface-enhanced Raman scattering sensors distinguishes early and advanced gastric cancer patients from healthy persons. *ACS Nano* **2016**, *10*, 8169–8179. [CrossRef]
142. Mason, E.A.; Kronstadt, B. Graham's laws of diffusion and effusion. *J. Chem. Educ.* **1967**, *44*, 740. [CrossRef]

143. Kim, S.; Kim, D.H.; Park, S.G. Highly sensitive and on-site NO₂ SERS sensors operated under ambient conditions. *Analyst* **2018**, *143*, 3006–3010. [[CrossRef](#)]
144. Zhang, Z.; Yu, W.; Wang, J.; Luo, D.; Qiao, X.Z.; Qin, X.Y.; Wang, T. Ultrasensitive surface-enhanced Raman scattering sensor of gaseous aldehydes as biomarkers of lung cancer on dendritic Ag nanocrystals. *Anal. Chem.* **2017**, *89*, 1416–1420. [[CrossRef](#)]
145. Qiao, X.Z.; Su, B.S.; Liu, C.; Song, Q.; Luo, D.; Mo, G.; Wang, T. Selective surface-enhanced Raman scattering for quantitative detection of lung cancer biomarkers in superparticle@MOF structure. *Adv. Mater.* **2018**, *30*, 1702275. [[CrossRef](#)]
146. Lawal, O.; Knobel, H.; Weda, H.; Bos, L.D.; Nijssen, T.M.E.; Goodacre, R.; Fowler, S.J. Volatile organic compound signature from co-culture of lung epithelial cell line with *Pseudomonas aeruginosa*. *Analyst* **2018**, *143*, 3148–3155. [[CrossRef](#)]
147. Lemfack, M.C.; Gohlke, B.O.; Toguem, S.M.T.; Preissner, S.; Piechulla, B.; Preissner, R. mVOC 2.0: A database of microbial volatiles. *Nucleic Acids Res.* **2018**, *46*, D1261–D1265. [[CrossRef](#)] [[PubMed](#)]
148. Lauridsen, R.K.; Sommer, L.M.; Johansen, H.K.; Rindzevicius, T.; Molin, S.; Jelsbak, L.; Engelsen, S.B.; Boisen, A. SERS detection of the biomarker hydrogen cyanide from *Pseudomonas aeruginosa* cultures isolated from cystic fibrosis patients. *Sci. Rep.* **2017**, *7*, 45264. [[CrossRef](#)] [[PubMed](#)]
149. Bos, L.D.J.; Sterk, P.J.; Schultz, M.J. Volatile metabolites of pathogens: A systematic review. *PLoS Pathog.* **2013**, *9*, e1003311. [[CrossRef](#)] [[PubMed](#)]
150. Park, K.J.; Wu, C.; Mercer-Smith, A.R.; Dodson, R.A.; Moersch, T.L.; Koonath, P.; Pipino, A.C.R.; Lu, H.W.; Yang, Y.W.; Sapirstein, V.S.; et al. Raman system for sensitive and selective identification of volatile organic compounds. *Sens. Actuator B Chem.* **2015**, *220*, 491–499. [[CrossRef](#)]
151. Junger, M.; Vautz, W.; Kuhns, M.; Hofmann, L.; Ulbricht, S.; Baumbach, J.I.; Quintel, M.; Perl, T. Ion mobility spectrometry for microbial volatile organic compounds: A new identification tool for human pathogenic bacteria. *Appl. Microbiol. Biotechnol.* **2012**, *93*, 2603–2614. [[CrossRef](#)] [[PubMed](#)]
152. Zhu, J.J.; Bean, H.D.; Wargo, M.J.; Leclair, L.W.; Hill, J.E. Detecting bacterial lung infections: In vivo evaluation of in vitro volatile fingerprints. *J. Breath Res.* **2013**, *7*, 016003. [[CrossRef](#)] [[PubMed](#)]
153. Kelly, J.; Patrick, R.; Patrick, S.; Bell, S.E.J. Surface-enhanced Raman spectroscopy for the detection of a metabolic product in the headspace above live bacterial cultures. *Angew. Chem.-Int. Ed.* **2018**, *57*, 15686–15690. [[CrossRef](#)] [[PubMed](#)]
154. Subaihi, A.; Muhamadali, H.; Mutter, S.T.; Blanch, E.; Ellis, D.I.; Goodacre, R. Quantitative detection of codeine in human plasma using surface-enhanced Raman scattering via adaptation of the isotopic labelling principle. *Analyst* **2017**, *142*, 1099–1105. [[CrossRef](#)]
155. Itoh, N.; Bell, S.E.J. High dilution surface-enhanced Raman spectroscopy for rapid determination of nicotine in e-liquids for electronic cigarettes. *Analyst* **2017**, *142*, 994–998. [[CrossRef](#)]
156. Westley, C.; Xu, Y.; Thilaganathan, B.; Carnell, A.J.; Turner, N.J.; Goodacre, R. Absolute quantification of uric acid in human urine using surface-enhanced Raman scattering with the standard addition method. *Anal. Chem.* **2017**, *89*, 2472–2477. [[CrossRef](#)]
157. Premasiri, W.R.; Lee, J.C.; Sauer-Budge, A.; Theberge, R.; Costello, C.E.; Ziegler, L.D. The biochemical origins of the surface-enhanced Raman spectra of bacteria: A metabolomics profiling by SERS. *Anal. Bioanal. Chem.* **2016**, *408*, 4631–4647. [[CrossRef](#)] [[PubMed](#)]
158. Kubryk, P.; Niessner, R.; Ivleva, N.P. The origin of the band at around 730 cm⁻¹ in the SERS spectra of bacteria: A stable isotope approach. *Analyst* **2016**, *141*, 2874–2878. [[CrossRef](#)] [[PubMed](#)]
159. Li, Y.Y.; Wei, Q.L.; Ma, F.; Li, X.; Liu, F.Y.; Zhou, M. Surface-enhanced Raman nanoparticles for tumor theranostics applications. *Acta Pharm. Sin. B* **2018**, *8*, 349–359. [[CrossRef](#)] [[PubMed](#)]
160. Baker, M.J.; Byrne, H.J.; Chalmers, J.; Gardner, P.; Goodacre, R.; Henderson, A.; Kazarian, S.G.; Martin, F.L.; Moger, J.; Stone, N.; et al. Clinical applications of infrared and Raman spectroscopy: state of play and future challenges. *Analyst* **2018**, *143*, 1735–1757. [[CrossRef](#)] [[PubMed](#)]
161. Neugebauer, U.; Schmid, U.; Baumann, K.; Ziebuhr, W.; Kozitskaya, S.; Deckert, V.; Schmitt, M.; Popp, J. Towards a detailed understanding of bacterial metabolism—Spectroscopic characterization of *Staphylococcus epidermidis*. *ChemPhysChem* **2007**, *8*, 124–137. [[CrossRef](#)] [[PubMed](#)]
162. Ashton, L.; Hogwood, C.E.M.; Tait, A.S.; Kuligowski, J.; Smales, C.M.; Bracewell, D.G.; Dickson, A.J.; Goodacre, R. UV resonance Raman spectroscopy: A process analytical tool for host cell DNA and RNA dynamics in mammalian cell lines. *J. Chem. Technol. Biotechnol.* **2015**, *90*, 237–243. [[CrossRef](#)]

163. Matousek, P.; Stone, N. Development of deep subsurface Raman spectroscopy for medical diagnosis and disease monitoring. *Chem. Soc. Rev.* **2016**, *45*, 1794–1802. [[CrossRef](#)]
164. Stone, N.; Kerssens, M.; Lloyd, G.R.; Faulds, K.; Graham, D.; Matousek, P. Surface-enhanced spatially offset Raman spectroscopic (SESORS) imaging—The next dimension. *Chem. Sci.* **2011**, *2*, 776–780. [[CrossRef](#)]
165. Matousek, P.; Stone, N. Recent advances in the development of Raman spectroscopy for deep non-invasive medical diagnosis. *J. Biophotonics* **2013**, *6*, 7–19. [[CrossRef](#)]
166. Nicolson, F.; Jamieson, L.E.; Mabbott, S.; Plakas, K.; Shand, N.C.; Detty, M.R.; Graham, D.; Faulds, K. Through tissue imaging of a live breast cancer tumour model using handheld surface-enhanced spatially offset resonance Raman spectroscopy (SESORRS). *Chem. Sci.* **2018**, *9*, 3788–3792. [[CrossRef](#)]
167. Zhang, Y.; Zhang, R.; Jiang, S.; Zhang, Y.; Dong, Z.C. Probing adsorption configurations of small molecules on surfaces by single-molecule tip-enhanced Raman spectroscopy. *ChemPhysChem* **2019**, *20*, 37–41. [[CrossRef](#)]
168. Berezin, S.; Aviv, Y.; Aviv, H.; Goldberg, E.; Tischler, Y.R. Replacing a century old technique—Modern spectroscopy can supplant Gram staining. *Sci. Rep.* **2017**, *7*, 3810. [[CrossRef](#)]
169. Ji, M.B.; Arbel, M.; Zhang, L.L.; Freudiger, C.W.; Hou, S.S.; Lin, D.D.; Yang, X.J.; Bacskai, B.J.; Xie, X.S. Label-free imaging of amyloid plaques in Alzheimer’s disease with stimulated Raman scattering microscopy. *Sci. Adv.* **2018**, *4*, eaat7715. [[CrossRef](#)]
170. Liao, C.S.; Wang, P.; Huang, C.Y.; Lin, P.; Eakins, G.; Bentley, R.T.; Liang, R.G.; Cheng, J.X. In vivo and in situ spectroscopic imaging by a handheld stimulated Raman scattering microscope. *ACS Photonics* **2018**, *5*, 947–954. [[CrossRef](#)]
171. Evans, C.L.; Xie, X.S. Coherent anti-Stokes Raman scattering microscopy: Chemical imaging for biology and medicine. *Annu. Rev. Anal. Chem.* **2008**, *1*, 883–909. [[CrossRef](#)]
172. Weng, S.; Xu, X.Y.; Li, J.S.; Wong, S.T.C. Combining deep learning and coherent anti-Stokes Raman scattering imaging for automated differential diagnosis of lung cancer. *J. Biomed. Opt.* **2017**, *22*, 106017. [[CrossRef](#)]



© 2019 by the authors. Licensee MDPI, Basel, Switzerland. This article is an open access article distributed under the terms and conditions of the Creative Commons Attribution (CC BY) license (<http://creativecommons.org/licenses/by/4.0/>).